Aalto University
School of Chemical
Technology

School of Chemical Technology
Master's Programme in Bioproduct Technology

Jean Buffiere

CELLULOSE DISSOLUTION IN NEAR- AND SUPERCRITICAL WATER FOR CELLO-OLIGOSACCHARIDES PRODUCTION

Master's thesis for the degree of Master of Science in Technology submitted for inspection, Espoo, 9 October, 2014.

Supervisor **Professor Herbert Sixta**

Instructor **M.Sc. Lasse Tolonen**

Aalto University
School of Chemi
Technology

Aalto University, P.O. BOX 11000, 00076 AALTO
www.aalto.fi

Abstract of master's thesis

Author	Jean Buffiere
Title of thesis	Cellulose dissolution in near- and supercritical water for cello-oligosaccharides production
Department	Department of Forest Products Technology
Professorship	Chemical Pulping Technology
Code of professorship	Puu-23
Thesis supervisor	Professor Herbert Sixta
Thesis advisor(s) / Thesis examiner(s)	M.Sc. Lasse Tolonen
Date	09.10.2014
Number of pages	69+15
Language	English

Abstract

Water-soluble cello-oligosaccharides and water-insoluble, low molecular weight cellulose polymers can be produced by controlled cellulose depolymerization of cellulose using supercritical water treatment. The products from the hydrolysis and dissolution of microcrystalline cellulose were investigated after a treatment at temperature range of 320 to 390 degrees Celsius and residence time range of 0.1 to 0.8 seconds. Four cellulosic product fractions were identified, quantified, and characterized using gravimetric and chromatographic techniques. The four fractions consisted of solid cellulosic residue, solid cellulosic precipitate, water-soluble cello-oligosaccharides, and water-soluble degradation products. The water-insoluble, low molecular mass cellulose polymers accounted for up to 25 percent of the total products. In addition, glucose and cello-oligosaccharides of degree of polymerization up to cellodecaose accounted for up to 65 percent of the total products. Furthermore, the water-soluble fraction was significantly purified using membrane ultrafiltration. These results show that the supercritical water treatment of microcrystalline cellulose is a fast and efficient method for producing both cello-oligomers and low molecular weight cellulose precipitate, which can be integrated into a full manufacturing process using downstream separation and purification methods.

Keywords supercritical water; cello-oligosaccharides; cellulose dissolution; cellulose hydrolysis; microcrystalline cellulose

FOREWORD

First, I would like to thank Lasse Tolonen for his high personal involvement and always wise advice throughout this project, and Prof. Herbert Sixta for kindly accepting me into his research group and supervising this thesis work.

I would also like to thank Rita Hatakka, Minna Mäenpää, and Myrtel Kåll for their experienced helping hands in analyzing my many samples.

I would like to express my gratitude to the Finnish Funding Agency for Technology and Innovations (TEKES) and the Finnish Bioeconomy Cluster (FIBIC) who funded this thesis work, as a part of the Future Biorefinery (FuBio) JR2 program.

Finally, my thanks go to Alina, whose patience, support and kindness never failed.

Espoo, 09.10.2014

Jean Buffiere

TABLE OF CONTENTS

LIST OF ABBREVIATIONS

CI	Crystallinity index
COS	Cello-oligosaccharide
DMF	Differential mass fraction
DP	Degree of polymerization
DP_w	Weight-average degree of polymerization
FTIR	Fourier-transform infrared spectroscopy
GPC	Gel permeation chromatography
HPAEC	High performance anion-exchange chromatography
LODP	Level-off degree of polymerization
MCC	Microcrystalline cellulose
MD	Molecular dynamics
MMD	Molecular mass distribution
M_n	Number-average molecular mass
M_w	Weight-average molecular mass
MWCO	Molecular weight cut-off
NMR	Nuclear magnetic resonance spectroscopy
PAD	Pulsed amperometric detection
PDI	Polydispersity index
$scCO_2$	Supercritical carbon dioxide
scH_2O	Supercritical water
SCWT	Supercritical water treatment
SEC	Size exclusion chromatography
SEM	Scanning electron microscopy
TO	Total organics
TOC	Total organic carbon
WAXS	Wide-angle X-ray scattering
X	Degree of conversion
XRD	X-ray diffraction
XRS	X-ray scattering

LIST OF FIGURES

1. INTRODUCTION

Cellulose is the most abundant bio-based polymer on Earth, and the main compound in all plant biomass species. Cellulose is a homopolymer of β(1→4)-linked D-anhydroglucopyranose units, forming linear chains with typical DPs (degrees of polymerization) of several thousand units. Linked with each other, these chains form cellulose microfibrils and fibers that are the main components of plant cell walls. The interest of numerous researchers in cellulose has been renewed over the past few decades, as cellulose is considered a potential starting material for producing a wide range of fuels, chemicals, and materials of renewable origin (Klemm et al., 2005).

The short-chain cellulose polymers, characterized with a DP between two and ten units, are commonly known as cello-oligosaccharides. High-potential applications of cello-oligosaccharides include their use as prebiotics and other food additives. Prebiotics refer to food ingredients that are not digested by human metabolism and have no energy intake. These oligosaccharides have traditionally been produced by acid-catalyzed or enzyme-catalyzed hydrolysis of cellulose (Akpinar 2002). However, such processes are relatively slow and require using concentrated chemicals or expensive enzyme complexes. Therefore, the evolution of the cello-oligosaccharides market and their related applications are today hindered by process limitations, thus requiring the development of an alternative, less restrictive method for controlled hydrolysis of cellulose.

Recently, hydrothermal treatment has been investigated as an alternative process for the controlled depolymerization of cellulose. Such hydrothermal treatment involves using nearcritical and supercritical water, that is water at high pressure and temperature around and above the critical point (374 °C and 221 bar), respectively. Under these conditions, microcrystalline cellulose is rapidly hydrolyzed and

dissolved with high yield into low molecular mass cellulose polymers and water-soluble cello-oligosaccharides (Sasaki et al. 1998).

However, several factors currently remain unclear, including both the mechanism driving cellulose degradation as well as the influence of the main operating parameters (temperature and residence time) on the product yield, and the formation of side products (Cantero et al. 2013). Furthermore, many of the potential applications of the cello-oligosaccharides require high purity of the product. While some fractionation methods have successfully been applied for the purification of oligosaccharides (Nabarlatz et al. 2007), no research has been focusing on assessing the feasibility of a combined system using supercritical water treatment and fractionation methods for producing cello-oligosaccharides.

In order to assess the viability of nearcritical and supercritical water treatment for the production of cello-oligosaccharides using microcrystalline cellulose, this thesis investigates the extent to which the treatment time and temperature affect the yield and molecular mass distribution of the product. Additionally, it assesses the feasibility of ultrafiltration for purifying oligomers mixtures. A simple techno-economic analysis is also performed in order to assess the potential viability of the process at more industrial scale.

The study is organized into four parts. Chapter 2 reviews the main available literature related to cellulose, the near- and supercritical treatment of cellulose, as well as the purification of oligosaccharides. Chapter 3 presents the supercritical bench, the experimental design, and the main analytical methods for product characterization. Chapter 4 describes the main experimental results obtained using the experimental bench and analyzed according to the methods presented in Chapter 3, and discusses their main implications. This chapter also presents a simple techno-economic feasibility of a pilot-scale, integrated system for producing cello-oligosaccharides based on the experimental results as the main design criteria.

2. LITERATURE REVIEW

2.1. CELLULOSE

Cellulose is an abundant bio-based polymer present in large quantities in all lignocellulosic biomass. The growth of lignocellulosic plants has been estimated to contribute to an equivalent annual production of cellulose up to 1.5 x 10^{12} tons globally, a large quantity of which is potentially available for producing a wide range of renewable, cellulose-based products (Klemm et al. 2005). In addition, its physical and chemical properties make cellulose a convenient and unique raw material for producing numerous types of products, including fibrous and composite materials, textiles, biofuels, fine chemicals, pharmaceuticals, and foodstuffs. More recently, cellulosic nanomaterials have been developed, which opened the way to a whole new range of cellulose-based products with excellent mechanical and gas barrier properties, such as nanocomposites, films, and functional packaging (Lavoine et al. 2012). Therefore, cellulose is believed to have a great role to play in the future as a non-food, ecological, and renewable raw material.

2.1.1. MOLECULAR AND MACROMOLECULAR STRUCTURE

Cellulose is a long, linear polymer composed of β,D-1,6-anhydroglucopyranose monomers, linked to each other by (1→4)-β-glycosidic bonds. The hydroxyl groups of cellulose are responsible for much of its general reactivity and internal cohesion between the single polymers chains. The individual cellulose polymer chains, which are believed to have a DP of around 10,000 in nature, are linked together by intermolecular hydrogen bonding and agglomerated in lignocellulosic biomass into bundles that are often referred to as microfibrils. The smallest of these bundles, the elementary fibrils, are believed to be composed of either 36 or 24 individual cellulose chains. Fernandes et al. (2011) reported X-ray scattering data consistent with a 24-chain model with a rectangular cross-section in spruce cellulose, but other models involving 36 chains and other cross-sectional geometries have been proposed. The microfibrils are the building blocks for lignocellulosic plant cells and their size varies according to the plant species as well as the measurement

methods, with typical widths of about 5 to 20 nm (Zugenmaier 2008). They are organized in the plant cell walls in a semi-crystalline arrangement, composed of more crystalline and more amorphous regions. When dead, the plant cells form macroscopic hollow fibers that can reach several millimeters in length in wood and several tens of micrometers in width. The fibers are a support tissue in plant stems and roots, which allows plants to grow vertically. In addition, they serve as a fluid transport matrix. Figure 1 shows a representation of the arrangement of the cellulose chains and fibrils in a plant cell wall.

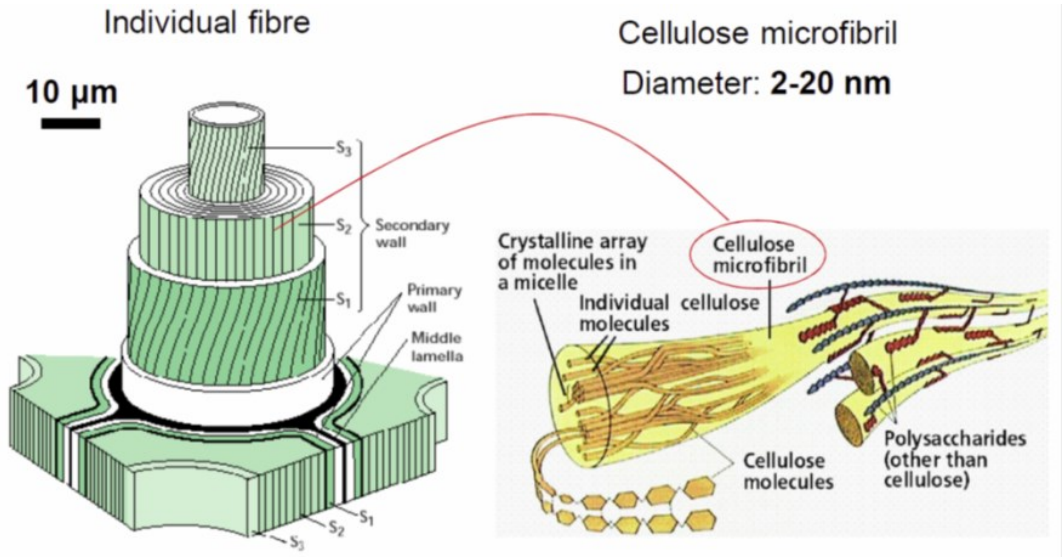

Figure 1. Molecular, supramolecular and fibrillar cellulose in the plant cell wall. (Kontturi 2013, adapted from Purves et al. 1994)

In addition to its supramolecular structure in the plant cell wall, cellulose is a polymorphic polymer. X-ray diffraction (XRD) studies, along with other experimental analyses, showed that cellulose polymer chains can bind with each other within the crystalline regions in microfibrils in at least three or four spatial arrangements, called allomorphs (Ciolacu and Popa 2010). The cellulose allomorphs are commonly referred to as cellulose I, cellulose II, cellulose III, and cellulose IV. The cellulose found in nature and in plant biomass is always the cellulose I allomorph. Two variations of cellulose I exist: cellulose I_α and I_β. These variations have been found to often coexist in nature but cellulose I_β composes most of the cellulose in terrestrial biomass. The cellulose II allomorph is observed after an artificial rearrangement of

the polymer chains has been performed. The cellulose I to cellulose II rearrangement can be caused either by the swelling (e.g., mercerization in concentrated sodium hydroxide) or the dissolution and regeneration of cellulose (further described in Section 2.1.3). The conversion from natural cellulose I to man-made cellulose II is an irreversible process, driven by the lower conformational energy of cellulose II. Therefore, all man-made non-functionalized cellulose products obtained by cellulose dissolution and regeneration, especially textile fibers, are composed of cellulose II. Two cellulose III allomorphs have been identified and have been prepared from cellulose I or cellulose II. The cellulose III_I and III_{II} allomorphs can be obtained through the reaction of ammonia or diamine with cellulose I or cellulose II, respectively. The thermal treatment of cellulose III in glycerol has been reported to form a fourth allomorph referred to as cellulose IV, but it is often considered a disordered variation of cellulose I rather than a distinct allomorph. Figure 2 shows representations of the special arrangement of cellulose monomers and polymer chains in cellulose I_α, I_β, II and III allomorphs and the corresponding free energies.

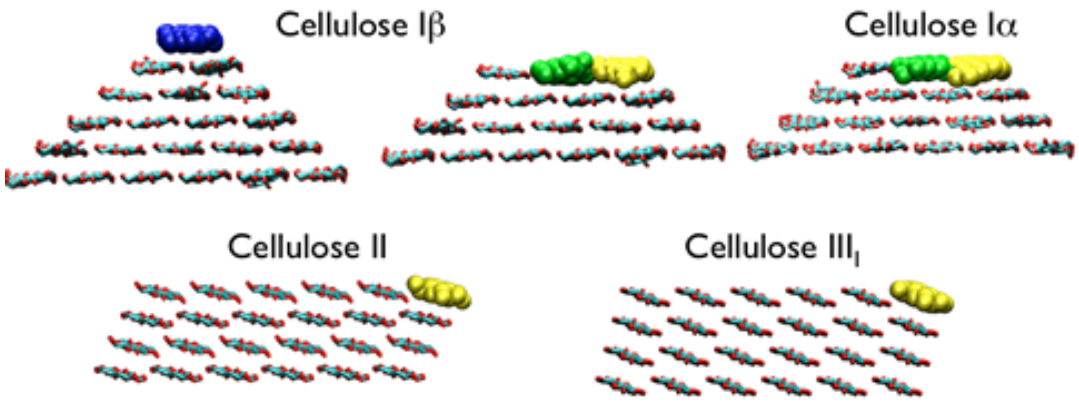

Figure 2. Spatial arrangement of cellulose I_α, I_β, II and III_I allomorphs. (Beckham 2014)

Despite the strong polarity and proticity of the hydroxyl group cellulose is a naturally water-insoluble material. One possible explanation for the thermodynamic stability of cellulose in water but also in most organic solvents is that the hydroxyl groups create strong internal cohesion forces within the cellulosic material.

Intramolecular hydrogen bonds (O_3-O_5) are responsible for the great stiffness of cellulose chains, while intermolecular hydrogen bonds (O_3-O_6 in cellulose I, O_2-O_6 in cellulose II) ensure the cohesion between the chains from the various layers within the microfibril (Nishiyama et al. 2003). The intermolecular hydrogen interactions are believed to play a role in the recalcitrance of natural cellulose, as proposed from the free energy observations obtained in molecular dynamics (MD) simulations (Bergenstråhle et al. 2010). In addition to intramolecular and intermolecular hydrogen bonds, it has been recently proposed that intersheet hydrogen bonds between the layers of polymer chains are also involved in the water-insoluble behavior of cellulose (Gross and Chu 2010). Furthermore, the amphiphilic character of cellulose in the plane of its pyranose ring has recently been suggested as an additional factor for internal cohesion of cellulose crystals (Medronho 2014). Figure 3 shows a representation of the intramolecular and intermolecular hydrogen interactions in cellulose I and cellulose II.

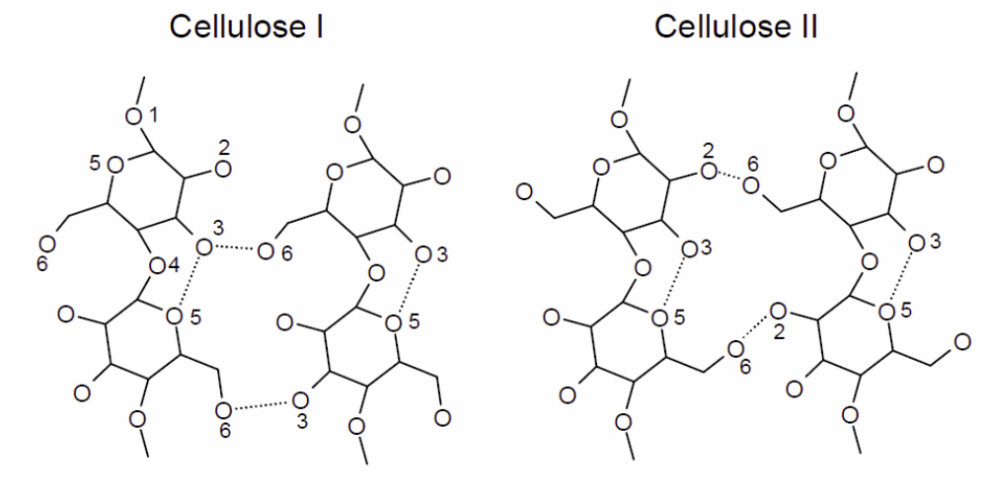

Figure 3. Hydrogen interactions in cellulose I and cellulose II.

(Kontturi et al. 2006)

Despite these strong interactions and the recalcitrance of its crystalline structure, natural cellulose is never a perfectly crystalline material. The study of cellulose diffraction patterns as well as other experimental observations indicated that cellulose chains are organized in microfibrils in a semi-crystalline arrangement; therefore, macroscopic cellulose is composed of both more crystalline regions (also

referred to as cellulose crystallites), as well as more less-ordered regions. The crystallinity index (CI), defined as the mass of crystallites per mass unit of cellulose sample, has been reported to vary significantly according to the cellulosic material, but also to the measurement method (Park et al. 2010). The semi-crystalline arrangement is responsible for mechanical and optical properties of the cellulose fibers, such as high strength and birefringence.

Several models have been developed in order to understand and describe the semi-crystalline arrangement of cellulose chains in microfibrils, in accordance with experimental results from XRD, electron micrograph and hydrolysis (further described in Section 2.1.5.) studies. One early model was proposed by Hearle (1958) and is commonly referred to as the fringed-fibrillar model. In the fringed-fibrillar arrangement short, numerous amorphous regions are randomly located among the crystallites. Figure 4 shows a schematic representation of the semi-crystalline arrangement of cellulose chains.

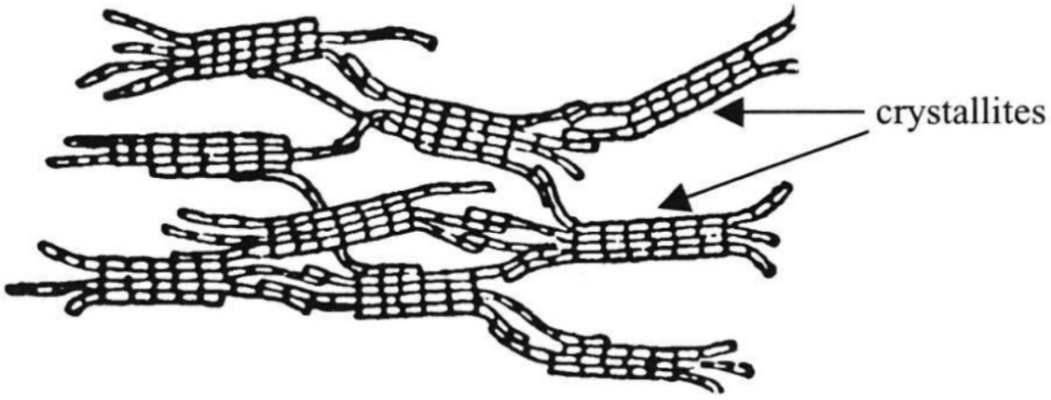

Figure 4. One fringed-fibrillar model for natural cellulose in microfibrils. (Gardner and Blackwell 1974)

The understanding of the molecular and supramolecular structure of cellulose, such as internal cohesion forces, surface reactivity, solubility, molecular mass distribution (MMD), and crystallinity are of particular importance in order to tailor the properties of cellulose-based materials, chemicals, and products to their desired end-uses.

2.1.2. USES

With a global estimated combined production of 400 million tons annually, cellulosic fibers are the starting material for the production of various materials and chemicals, the largest of which are paper and board (Sixta 2006). The fibers also traditionally serve as a raw material for producing derived fibrous products, such as filters, absorbent materials, and various packaging solutions. For these applications the mechanical strength of cellulose needs to be high, which translates into high DP for cellulose polymer chains. Therefore, one main challenge for producing high performance cellulose-based materials is to limit the degradation of cellulose during the fractionation of carbohydrates from lignocellulosic raw materials (pulping), but also during the subsequent manufacturing steps (e.g., bleaching, pressing, or drying). In addition to the traditional native fibrous-based materials, two novel categories of nano-sized cellulose raw materials have recently been developed, namely nanofibrillar cellulose and nanocrystalline cellulose. These two platform materials have demonstrated high potential and unique properties that are suitable for a various range of uses that include nanocomposite materials, intelligent packaging, and rheology control (Lavoine et al. 2012).

Several other uses of cellulose require the dissolution and the regeneration of cellulose polymer chains into cellulose II. The dissolution of cellulose is a tedious operation, and only a limited number of solvents today are able to dissolve cellulose efficiently, with or without chemical derivatization (further described in Section 2.1.4.). The regeneration of cellulose generally involves the addition of an antisolvent and is mostly performed using water. The properties of the products obtained by such processes can be extensively tailored to their final applications, which include man-made fibers, films, surfactants, pharmaceuticals, and other derivative polymeric compounds. In most cases the high DP of cellulose remains an important parameter for the properties of the final products as well as cellulose purity, although adjusting the DP allows producing dissolved pulps solutions with various viscosity grades (Olsson and Westman 2013). Dissolving-grade cellulose (dissolving pulp) generally requires specific fractionation and purification processes,

such as acid sulfite pulping combined with a caustic extraction step in order to efficiently remove the residual lignin and hemicelluloses from the pulp.

A third category of cellulose-based products involves the depolymerization of cellulose into monomeric glucose and further conversion of glucose into other chemicals. Glucose of lignocellulosic origin is produced from non-food raw materials; therefore, it is considered a more sustainable product than glucose produced from edible plants such as corn and potatoes. Cellulose depolymerization is performed in water by catalytic hydrolysis, which cleaves the glycosidic bonds of the cellulose chains. The hydrolysis reaction is catalyzed using enzymes (enzymatic hydrolysis) or acids (acid-catalyzed hydrolysis, further described in Section 2.1.5.). The main product from glucose is ethanol, which is today being produced at increasing scale in order to replace glucose of food origin, and which global production has been estimated to reach 100 billion liters by 2015 annually (Taherzadeh and Karimi 2007). Ethanol is obtained through fermentation of glucose, but numerous other valuable fuels and platform chemicals can be produced through cellulose hydrolysis and glucose conversion, including levulinic acid and 5-HMF. The main reported challenge for cellulose conversion to monomeric glucose is the limited commercial viability of its process due to high costs of enzymes and acids as well as limited hydrolysis yield, hindered by the limited accessibility of the glycosidic bonds because of the crystallinity of cellulose. In addition, the presence of residual lignin and other aromatic compounds from the original biomass in cellulose can inhibit the activity of enzymes and further reduce the hydrolysis efficiency (Yang et al. 2011).

Finally, a fourth category of cellulose products can be identified, which results from the controlled, partial depolymerization of cellulose using similar hydrolysis techniques as for cellulosic glucose production. These products include microcrystalline cellulose (further described in Section 2.1.6.), cellulose oligosaccharides (COS, also referred to as cello-oligomers, and further described in Section 2.2.), and other short-chain cellulose materials. A general challenge in producing low molecular mass cellulose polymers is the lack of selectivity of the

processes, leading to products having wide MMDs and high polydispersity indexes (PDIs). In addition, the polymers are difficult to fractionate according to their DP. Potential applications of such products make use of the chemical inertness and rheological properties of cellulosic materials, as well as their reported positive effects on human digestion and health; they include prebiotics and other food additives (Akpinar and Penner 2004). However, the current production and purification methods seem to be inadequate for large-scale production from cellulose; therefore, their value as commercial products is today limited.

2.1.3. DISSOLUTION AND REGENERATION

The dissolution of natural cellulose is a difficult operation. The high DP of cellulose, the strong internal cohesion of its chains, as well as its relatively inaccessible semi-crystalline structure result in a strong resistance to most conventional aqueous and organic solvents. Molecular dynamics (MD) simulations have been performed in order to investigate the insolubility behavior of cellulose in water. These studies have sustained the insolubility behavior of cellulose in ambient water due to interactions within cellulose chains that thermodynamically favor its crystal conformation (Bergenstråhle et al. 2010).

The swelling of cellulose in solvents, such as sodium hydroxide, NMMO and some ionic liquids has been experimentally observed either as a steady state (intracrystalline swelling) or as the first step prior to solvation (intercrystalline swelling) depending on the experimental conditions. Intracrystalline swelling does not affect the cellulose crystallites while intercrystalline swelling breaks down its crystalline structure. A ballooning effect has been revealed in fibers with NMMO under certain limiting operating conditions. The ballooning has been explained as the result of the swelling and dissolution of the secondary cell wall while the primary wall remained swollen and undissolved (Navard and Cuissinat 2006). In addition, swelling in sodium hydroxide has been extensively reported as causing the conversion of the cellulose crystallites from cellulose I to cellulose II, and is largely

used in the mercerization process for increasing the surface reactivity of textile fibers (Olsson and Westman 2013).

One alternative method to overcome the insolubility of cellulose is its chemical derivatization. Cellulose can be made water-soluble by introducing polar, steric chemical functions covalently bound to the hydroxyl groups of cellulose by ether or ester linkages which hinder the initial hydrogen bonding pattern in cellulose. The water-soluble cellulose derivatives include cellulose acetate, nitrate, xanthate, as well as methyl ether and carboxymethyl cellulose. The water affinity of the products depends on the degree of substitution of the derivatizing function. These compounds are widely used for various large-scale commercial applications, such as textile fibers, films, and surfactants.

Only a limited number of solvents have been found capable of dissolving cellulose without chemical derivatization and are today available. These non-derivatizing solvents can be sorted into three categories according to the number of components in the solvent system. Tricomponent cellulose solvents include the H_2O-NaOH-urea and the NH_3-SO_2-DMSO systems. Bicomponent solvents include the DMAc-LiCl, the Cu(II)-EDA, the NMMO, and the H_2O-NaOH systems. Monocomponent solvents include some of the increasingly investigated and popular ionic liquids, some of which have been shown able to rapidly and efficiently dissolve cellulose (Zhu et al. 2006).

In addition to the difficulty of finding suitable cellulose solvents, and with the exception of ionic liquids, the dissolution process of cellulose is in most cases a slow process. No general theory has been developed for cellulose solvent parameters, and new solvents are mainly found experimentally. However, a three-parameter empirical model commonly referred to as the Kamlet-Taft model has been developed, which considers the acidity, basicity and polarizability of the solvents (parameters α, β, and π^*, respectively). The model showed that the parameters for the already known cellulose solvents are all located within a limited range, especially regarding the value of the difference $\alpha - \beta$ (Hauru et al. 2012).

2.1.4. HYDROLYSIS

Cellulose depolymerization can be achieved by catalytic hydrolysis of its glycosidic bonds. Cellulose hydrolysis can be classified into two categories related to the nature of the catalyst: enzymatic-catalyzed hydrolysis and acid-catalyzed hydrolysis (Wyman et al. 2004). Enzymatic hydrolysis is performed in aqueous systems using specific cellulase complexes. Enzymatic hydrolysis has mainly been investigated for the purpose of converting cellulose and other C_6 sugars into glucose for further fermentation into ethanol or other chemicals (Yang et al. 2011). Homogeneous acid-catalyzed hydrolysis is performed in aqueous system using strong acid such as sulfuric acid, hydrochloric acid, formic acid, or a mixture of these acids (Kupiainen et al. 2012). The reaction can be performed either at low temperature, with high acid concentration and long reaction time (concentrated acid hydrolysis), or at high temperature, with low acid concentration and short reaction time (diluted acid hydrolysis). While concentrated hydrolysis gives higher glucose yields (typical maximum value about 90 % of the theoretical maximum yield), handling concentrated acid solutions can result in more corrosion and safety issues (Taherzadeh and Karimi 2007). In addition, heterogeneous acid hydrolysis has been increasingly reported as an alternative method for hydrolyzing cellulose with lower problems related to wastewater treatment and catalyst recycling. Such processes use solid catalysts such as sulfonated carbonaceous based acids, polymer based acids and magnetic solid acids, but currently yield lower glucose fractions compared to homogeneous acid-catalyzed or enzymatic hydrolysis (Huang and Fu 2013).

The random depolymerization of an infinitely long, linear polymer can be described as the same way as the random polymerization by condensation of linear polymers, the former phenomenon being the opposite as the latter. Flory (1936) developed a theoretical model which takes into account the number of bond formation (or cleavage) in order to statistically predict the molecular length distribution of the final polymer. The equation describing this model is today commonly referred to as the Flory-Schulz formula. Assuming that acid-hydrolysis of cellulose follows a random mechanism the molar mass distribution of partially hydrolyzed cellulose

can be described using the Flory-Schulz equation. Equation 1 shows the Flory-Schulz formula giving the differential mass fraction (DMF) of a randomly depolymerized, infinitely long, linear polymer as a function of the DP and two equation parameters a and b.

$$DMF = a \times DP \times (1 - b)^{DP-1} \quad (1)$$

However, the semi-crystalline structure of natural cellulose as well as the strong cohesion and the limited accessibility of the cellulose chains in the more crystalline regions significantly affect the hydrolysis of cellulose, especially when using acid catalysts. Evidence of the semi-crystalline structure has been extensively reported from experimental hydrolysis studies, where the degradation of cellulose happened in two phases. At first the average DP of cellulose first showed a linear and relatively rapid decrease over time. However, after a given reaction time the rate of depolymerization dramatically decreased and the average DP reached a plateau value. Series of experiments performed at various reaction conditions (temperature, acid concentration, cellulose consistency) showed different reaction speeds, but a similar end-reaction plateau value for cellulose DP, which is commonly referred to as the level-off degree of polymerization (LODP). However, even after reaching the LODP a linear weight loss in the residual cellulose was reported, indicating that the hydrolysis of cellulose continued without significantly affecting the overall DP of cellulose (Millet et al. 1954).

Sharples (1957) developed a two-stage model describing the acid-catalyzed hydrolysis of cellulose that is compatible with these experimental observations. The first stage is a depolymerization of the more accessible, randomly distributed amorphous regions of cellulose, resulting in a fast decrease in average DP. The resulting crystallites are relatively protected from side glycosidic bond cleavage. Therefore, the second hydrolysis stage on the model only takes place at the non-reducing end of the cellulose chains, which are peeled off, only resulting in a slight decrease in the overall DP of cellulose. However, experimental kinetic results may have showed the limit of the two-stage model when applied to cellulose I (Lin et al.

1993). Figure 5 shows a representation of the original two-stage hydrolysis model, with the two steps represented as 1 and 2, respectively.

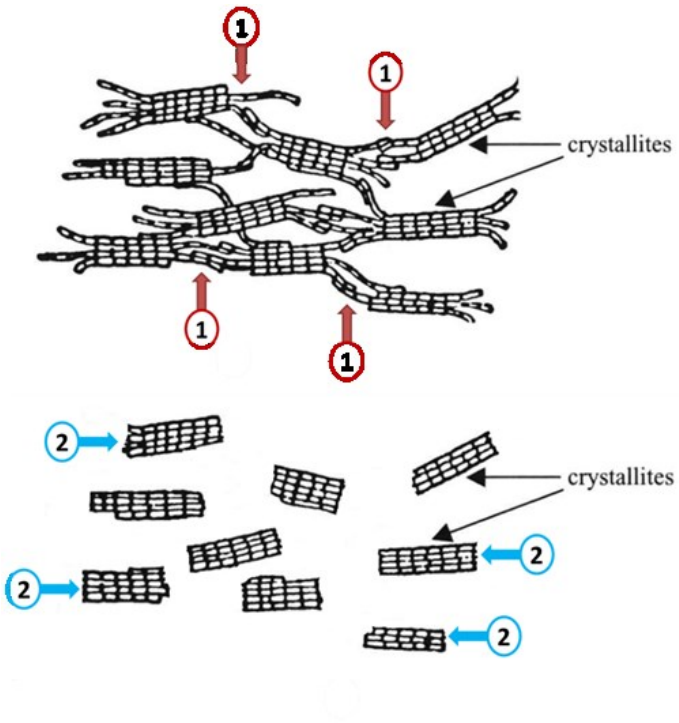

Figure 5. Two-stage cellulose hydrolysis model.
(Adapted from Gardner and Blackwell 1974)

Therefore, the complete depolymerization of cellulose into glucose monomers is a relatively long and difficult operation, due to the existence of the LODP as well as the further degradation of glucose under severe treatment conditions. Therefore, several pretreatments have been developed in order to increase the accessibility of cellulose prior to its depolymerization, including various chemical, biological, mechanical, and thermal approaches (Yang and Wyman 2008). However, acid-catalyzed hydrolysis is an effective method for producing microcrystalline cellulose (MCC).

2.1.5. MICROCRYSTALLINE CELLULOSE

Microcrystalline cellulose is high purity, partially hydrolyzed cellulose powder with a high content in cellulose crystallites. MCC is typically obtained after partial dilute acid-catalyzed hydrolysis of the amorphous regions in natural cellulose to reach its

LODP. Therefore, MCC is mainly composed of cellulose crystallites. Starting materials, such as cotton linters or dissolving-grade pulp are suitable for producing MCC due to their high initial purity in cellulose. The manufacturing process typically includes steps, such as alkaline pretreatment, acid-catalyzed hydrolysis at moderate temperature, washing, and spray drying (Zugenmaier 2008). MCC can also be produced by other methods, including controlled enzymatic hydrolysis (Stupińska et al. 2007). Cellulose purity above 97 % in MCC has been reported. The main characteristics of commercial MCC are the particle size typically between 20 and 80 µm, its average DP_w typically from 100 to 400, and its crystallinity index (CI) typically from 60 to 80 % obtained by XRD (Nada et al. 2009). The CI values indicate that a significant portion of MCC is composed of imperfect crystallites. Park et al. (2010) reported significant discrepancies between the crystallinity values when measured by different methods. MCC is today widely used as a cellulose model substrate (e.g., in thin-layer chromatography or for assessing enzymatic activity), and also has applications as excipient or additive in the pharmaceutical, medical, and food industries.

2.2. CELLO-OLIGOSACCHARIDES

Cello-oligosaccharides (COSs) are individual cellulose polymer chains with a short DP. The generally accepted definition for COSs includes oligomers composed of two to ten anhydroglucose units, but the upper limit for the DP of COSs varies among publications from seven to twelve units. In biochemistry COSs are also commonly referred to as cellodextrins. The nomenclature for COSs is presented in Appendix A.

2.2.1. SOLUBILITY IN WATER

Unlike natural cellulose, most COSs are considerably soluble in pure, ambient water. The solubility limit has been proposed for cellooctaose (DP eight), above which the solubility of the COSs is considered negligible. However, experimental solubility studies using TOC have been performed for the shorter COSs in ambient water, and reported that the solubility value rapidly decreases with increasing DP of the COSs

(Gray et al. 2003). Anion-exchange chromatography of mixtures of COSs with high DP range showed that traces of COSs with DP up to 16 can be found in ambient water after supercritical hydrolysis and stabilization of the product for 48 hours (Yu and Wu 2009).

2.2.2. PRODUCTION PATHWAYS

Cello-oligosaccharides are difficult to obtain in large quantities. Two main pathways have been developed, which allow producing them in small quantities: by cellulose depolymerization, and by synthesis. Cellulose depolymerization can be either chemical or enzymatic, and involves catalytic hydrolysis (described in Section 2.1.5). The product of partial hydrolysis includes glucose and cellulose polymer chains of various lengths, including significant amounts of COSs. A significant yield of COSs mixture has been reported from the treatment of MCC in fuming hydrochloric acid (Huebner et al. 1978). As an alternative to fuming hydrochloric acid, the treatment of MCC with a mixture of concentrated hydrochloric acid and concentrated sulfuric acid led to a yield of 20 % in COSs from DP 3 (cellotriose) to DP 6 (cellohexaose) (Zhang and Lynd 2003). The acetolysis of cellulose followed by deacetylation has also been a reference method for COSs production, which can also be produced from partial enzymatic hydrolysis using a cellulase enzyme complex and an inhibitor of the enzyme responsible for glycosidic bond cleavage. Final concentrations of COSs with DP 2 to 4 in the range of several grams per liter of supernatant product phase have been reported using this method (Akpinar 2002).

The second possible pathway for producing COSs is the synthesis. Both chemical and biochemical methods have been successfully developed to produce COSs. Chemically, the Koenigs-Knorr glycosylation of glucose pentaacetate using hydrobromic acid in glacial acetic acid followed by deacetylation in methanol led to the formation of a glycosidic bond; therefore, this reaction allowed producing COSs from glucose. Biochemical synthesis of COSs was achieved using specific enzymes such as glycoside hydrolases, and a glycosidic donor such as and glycoside fluoride. High yield and high COSs selectivity were reported using this method, and

alternative synthesis pathways with overall high efficiencies have been developed as well (Akpinar 2002).

2.2.3. PURIFICATION AND FRACTIONATION

Regardless of the production method, cello-oligosaccharides are generally obtained at first in a dilute aqueous medium containing various other components, such as acids, enzymes, or residual cellulose. Therefore, in order to be further used in specific applications, the COSs must be purified and isolated, or fractionated. Some of these applications (further described in Section 2.2.5.) require the complete fractionation of COSs into pure, single DP components, while other uses can accommodate with a mixture of components with various DPs and only require the removal of contaminants.

Several purification methods have been applied to the purification of COSs, including precipitation and evaporation, ion-exchange, and ultrafiltration. A yield of 10 % in COSs has been reported from acid-catalyzed hydrolysis of MCC using several consecutive steps of acetone precipitation and evaporation in a rotary evaporator (Russell 1985). Successful precipitation has also been reported in ethanol and 1-propanol (Akpinar and Penner 2004). Adsorption on activated carbon as well as ion-exchange columns, such as carbon-celite column (calcium or magnesium acid silicate column have also been used) are also able to isolate the COSs from the solutions (Akpinar 2002).

In addition, ultrafiltration has been proposed as an alternative method and was successfully applied for both removing low molecular mass contaminants, and concentrating solutions containing mixtures of oligosaccharides. Goulas et al. (2002) reported yields in the range between 60 % and 95 % for di- and trisaccharides in cross-flow continuous diafiltration. Similar yields were obtained using a dead-end filtration cell system and various types of membranes, which demonstrated the potential of ultrafiltration for purifying and concentrating mixtures of oligosaccharides (Goulas et al. 2003). Nabarlatz et al. (2007) successfully purified a mixture containing oligosaccharides and suggested that the oligomers can be

separated using an ultrafiltration sequence comprising several membranes using various pore sizes. In addition, the authors also reported good resistance to fouling for all the tested membranes.

Furthermore, the fractionation of COS mixtures according to their DP is possible using several chromatographic techniques. A gradient elution with an ethanol-water phase, applied to the adsorbed COSs on a carbon-celite column, was able to fractionate the COSs according to their DP (Huebner et al. 1978). Gel permeation chromatography (GPC) was applied with a moderate efficiency, while ion-exchange chromatography combined with acetone precipitation and another chromatography were able to fully fractionate COSs up to DP 6 with purities of the final fractions in the range of 95 to 99 %, with a production capacity of several hundreds of mg per day, and with water as the sole solvent (Zhang and Lynd 2003).

2.2.4. APPLICATIONS

Despite the current limitations in producing cello-oligosaccharides at a large scale, a number of potential applications have been identified for COSs. These applications include the use of COSs as food additives, analytic model compounds of cellulose, model substrate for cellulase activity, and raw material for chemical functionalization. COSs are prebiotics, that is, non-digestible fiber compounds. Adding significant amounts of COSs as prebiotics to food has been found to have a positive effect on health, with identified functions, such as lowering cholesterol levels and preventing diabetes and obesity. In addition, pure COSs have been used for characterization of the activity of cellulase enzymes, and serve as standard compounds for ion-exchange chromatography calibration. Furthermore, the accessibility of the reducing-end of the COSs promotes their chemical functionalization (Akpinar 2002). Other possible applications are likely to be found for cello-oligosaccharides in the future but the lack of cost-effective scalable production method is currently the limiting factor of their development.

2.3. SUPERCRITICAL WATER TREATMENT OF CELLULOSE

A supercritical fluid is any substance at a temperature and pressure above its critical point. The existence of the critical point and the supercritical fluid phase of chemical compounds was discovered in 1822 by the French engineer Charles Cagniard de la Tour. However, the use of supercritical fluids for industrial applications was only made possible by recent advance in science and engineering, such as materials science, mechanical engineering and chemical engineering, where designs and processes must be optimized to withstand high operating temperatures and pressures.

Under supercritical conditions distinct liquid and gas phases do not exist. The physical and chemical properties of the supercritical fluid typically considerably differ as compared to the properties of the liquid and gaseous phases. Above in the vicinity of the critical point (near-critical conditions) physical properties, such as density, viscosity, and dielectric constant reach values that are impossible to reach under ambient conditions. In addition, the near- or supercritical conditions modify the solvent properties of the fluids. For these reasons supercritical fluids have received much interest in the past decades and several near-industrial or industrial applications have been developed, mainly for uses as environmentally-friendly solvents or for waste treatment purposes (Galkin and Lunin 2005).

Two supercritical fluids have received special attention as of today: supercritical carbon dioxide ($scCO_2$) and supercritical water (scH_2O). The main applications for these two fluids include destruction of industrial waste, dry-cleaning, chemical extraction, chromatography, and chemical reactions gasification, oxidation, and hydrolysis. Many of these applications are based on the enhanced solvent properties of the fluids under supercritical conditions; they have traditionally been performed using hazardous, expensive organic solvents. Therefore, supercritical fluids are often regarded as promising reaction media in green chemistry, despite the high capital costs inherent to high operating temperatures and pressures and the limited freedom in adjusting the properties of the fluid (Shaw et al. 1991).

2.3.1. SUPERCRITICAL WATER

The supercritical phase of water is located above its critical point, at T = 374 ˚C and P = 221 bar, as depicted in Figure 6. These conditions are relatively high compared to the critical point of carbon dioxide (T = 31.1 °C and Pc = 73.9 bar), which is mainly due to the high intermolecular cohesion forces between the water molecules.

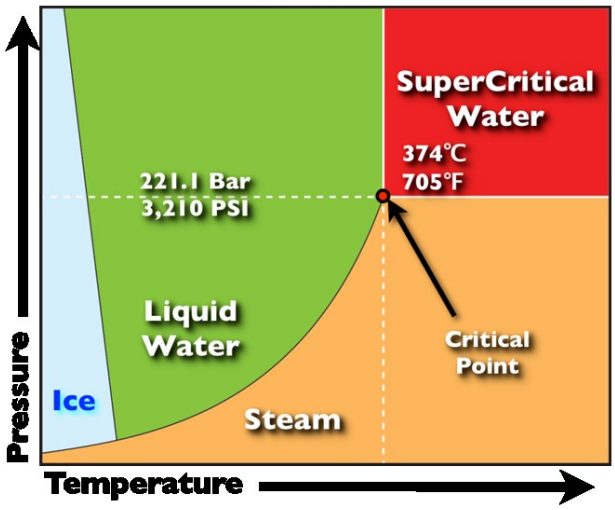

Figure 6. Phase diagram of water.

(Kamler and Soria 2012)

The study of water as a function of temperature and pressure revealed significant changes in its main properties in the vicinity and above the critical point, including density, viscosity, dielectric constant, and ion product (Lemmon et al., Uematsu and Frank 1980, Marshall and Frank 1981). In addition to these physical properties, experimental studies showed that near- and supercritical conditions led to a decrease in hydrogen bonding as well as a modification of ionic and nonpolar repelling behavior of water. Therefore, water was shown able to dissolved nonpolar compounds, such as hydrocarbons, while most salts become insoluble in supercritical water. In addition, the properties undergo significant changes already at near-critical conditions, which make near-critical water also an interesting medium for chemical reactions and an interesting solvent (Galkin and Lunin 2005). Figure 7 shows the variation of the density, dielectric constant as well as hydrocarbon and inorganic solubility of water as a function of temperature.

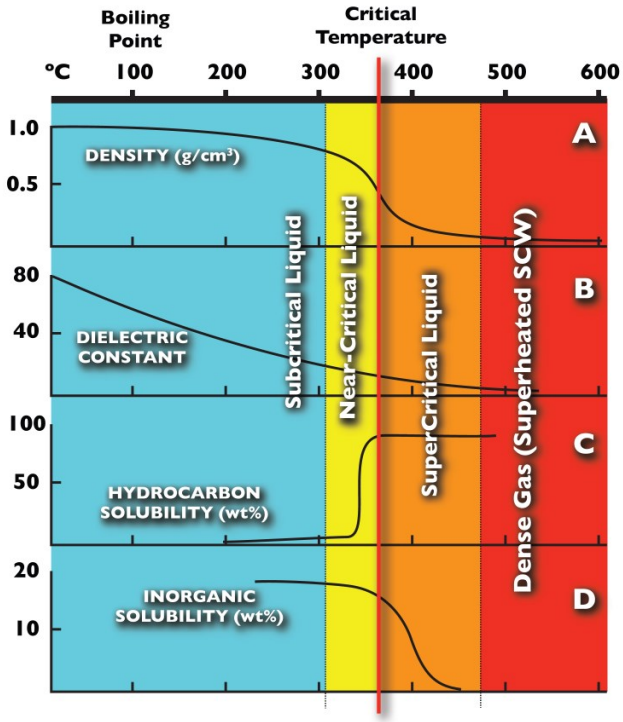

Figure 7. Properties of water at 250 bars as a function of temperature. (Kamler and Soria 2012)

2.3.2. SUPERCRITICAL TREATMENT OF CELLULOSIC BIOMASS

Supercritical water treatment (SCWT) of cellulosic biomass refers to a range of treatments applied to the whole lignocellulosic biomass in a wet environment using water under supercritical conditions. SCWT of biomass degrades the lignocellulosic material, either to fractionate the raw material into its individual components (e.g., cellulose, hemicelluloses, lignin), or to convert it by direct thermochemical conversion into chemicals, such as hydrogen, methane, as well as other water-soluble and gaseous compounds. This type of process is also referred to as supercritical hydrotreatment or supercritical gasification (Peterson et al. 2008). One main advantage of SCWT of biomass for thermochemical conversion to fuels is that it uses water as a reaction medium. Therefore, the biomass requires no preliminary drying, which is generally an energy-intensive step.

SCWT has been investigated for hydrolyzing the fermentable sugars of biomass. In this case, the carbohydrates are depolymerized and solubilized while lignin and

other hydrophobic compounds remain insoluble. The process can be performed in two steps for increased conversion efficiency and extraction of the non-fermentable C_5 sugars. Therefore, SCWT is believed to be an efficient, scalable way of producing glucose for further fermentation into cellulosic ethanol. This method has several advantages compared to the traditional combined pretreatment followed by the enzymatic hydrolysis of lignocellulosic biomass, including its treatment rapidity as well as the absence of potentially hazardous solvents and expensive reactants (Sinag et al. 2009). From more severe SCWTs of biomass with longer residence times the formation of a significant amount of methane, hydrogen and other gaseous compounds has been observed. Therefore, supercritical water is believed to be a possible environmentally-friendly pathway for producing both condensable and non-condensable gaseous fuels.

2.3.3. SUPERCRITICAL TREATMENT OF MICROCRYSTALLINE CELLULOSE

The behavior and degradation of microcrystalline cellulose in scH_2O has been increasingly investigated in the last twenty years, in parallel with SCWT studies applied to the whole lignocellulosic biomass. As far as MCC is concerned, due to the novelty of the treatment and the use of MCC as a cellulose model compound, the focus of research studies has in most cases been more on theoretical aspects than on commercial applications. Studies were conducted in order to understand the kinetics and mechanisms for cellulose degradation, the formation of the various observed product fractions, as well as the role of supercritical water in cellulose dissolution and hydrolysis.

Sasaki et Al. (1998) studied the non-catalyzed hydrothermal reaction of microcrystalline cellulose under supercritical water conditions in a plug-flow reactor system. The system had fixed flows and variable reactor length to adjust the reaction time, and performed experiments at 250 bars and at a temperature range of 290 to 400 °C. The reaction times ranged from 0.05 to 10 s. It was observed that under these conditions MCC was rapidly degraded and converted into monomeric sugars, cello-oligomers, and various degradation products, such as fructose,

erythrose, glyceraldehyde, 5-HFM and other acids. The reported cellulose conversion yield for these products reached up to 75 % with a residence time in the order of a few seconds only. Sasaki et al. (1998) proposed a two-step general mechanism involving the hydrolysis of cellulose into glucose and water-soluble cello-oligosaccharides up to DP6, followed by further decomposition of these compounds into the identified degradation products.

A kinetic model was developed assuming a grain model for MCC with a surface reaction and a first order reaction kinetics. The model showed that the rate of cellulose hydrolysis considerably increased around and above the critical temperature, thus increasing the proportion of hydrolysis products at supercritical temperatures compared to the formation of degradation products. These results were confirmed by visual observations using a diamond anvil cell, showing that increased reaction temperatures lead to the more rapid disappearance of the MCC particles already at near-critical temperatures, which also suggested that the hydrolysis could be taking place in homogenous medium, and therefore that scH_2O is able to dissolve MCC (Sasaki et al. 2000). In addition, the authors observed the formation of solid precipitation products in most samples, which were initially transparent, after a cooling-down period of 30 to 120 min. FTIR spectroscopy suggested that these precipitation products were relatively high DP cellulose oligomers that were insoluble in ambient water.

Several other research groups performed similar experiments with comparable plug-flow reactor systems and obtained similar results. Ehara and Saka (2002) compared the SCWT products obtained with a batch-type and a flow-type reactor, and concluded that continuous reactors give lower amounts of degradation products; therefore, they are more suitable for hydrolyzing cellulose into glucose and COSs. These authors tested the first-order kinetic model mentioned previously using similar assumptions and obtained comparable results. This approach was repeated in other publications (Cantero et al. 2013). Figure 8 shows a compilation of the kinetic constants for cellulose hydrolysis obtained by various research groups assuming a first order hydrolysis reaction.

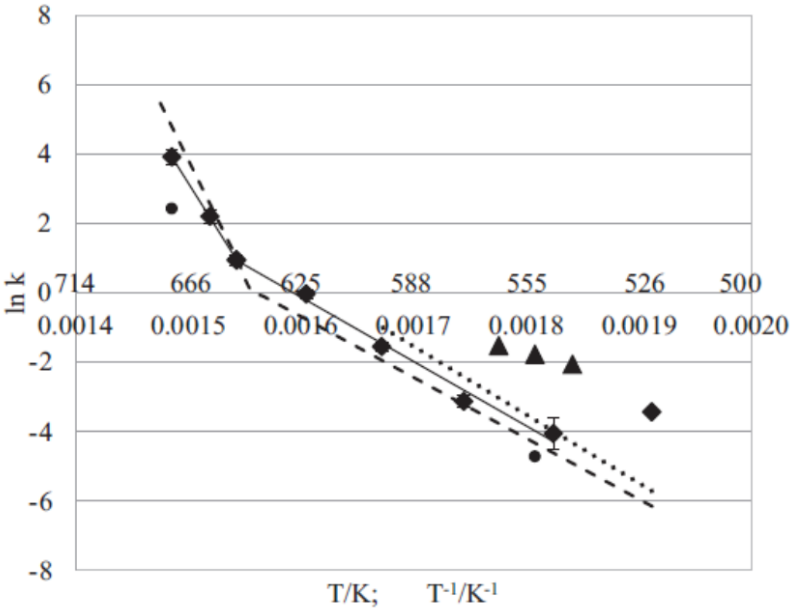

Figure 8. Cellulose decomposition rates from literature.

(Cantero et al. 2013)

In addition to glucose, various degradation products and water-soluble COSs with DPs up to 12, Ehara and Saka (2002) also observed the slow precipitation of water-insoluble cellulose polymers and assumed a wide MMD in the DP range of 13 to 100, therefore indicating that cellulose chains with such DPs are soluble in supercritical water. Furthermore, XRD showed that the precipitates were cellulose II, typically obtained after dissolution and regeneration of cellulose, and later on confirmed by other groups (Sasaki et al. 2003). Therefore, in addition to producing glucose and water-soluble COSs, the SCWT of MCC is also a process capable of producing low DP cellulose II.

Deguchi et al. (2006) obtained in-situ microscopic images of the degradation of MCC in subcritical and near-critical water and observed a loss in cellulose birefringence at temperatures higher than 320 °C, as well as a gain in transparency of the MCC. The authors proposed that cellulose is undergoing a crystalline-to-amorphous transition in SCWT, similar to the commonly observed phenomenon of starch gelatinization (Deguchi et al. 2008). They also underlined the importance of water molecules in

the transition, as no such change in crystallinity was observed in ethanol under similar conditions.

The hydrolysis products of MCC in subcritical water and the precipitation of the higher DP oligomers were investigated by Yu and Wu (2009). High-performance anion exchange chromatography with pulsed amperometric detection (HPAEC-PAD) calibrated with standard oligomer compounds was proved an efficient method for characterization of the COSs. This technique was capable of both quantifying the COSs with DPs up to 5 and identifying the COSs with DPs up to about 30. The authors showed that COSs with DP > 6 rapidly become supersaturated in ambient water, slowly precipitate into cellulose II allomorph, and form the precipitate fraction. In addition, it was found that although the precipitation starts immediately after sample production, it is a slow process and can still occur during a period of up to five days. These observations concur with previous MMD analyses of the precipitate fraction obtained by viscosimetry. Sasaki et al. (2004) reported a viscosity-average DP of precipitate ranging from about 30 to about 50.

Recently, Tolonen et al. (2011) observed a LODP phenomenon for the treatment of microcrystalline cellulose in subcritical water, as cellulose was degraded with only a limited decrease in the DP. In addition, X-ray scattering (XRS) and nuclear magnetic resonance (NMR) spectroscopy showed that the crystallinity of the residual cellulose only presented a slight change in crystallinity throughout the treatment. The authors proposed that the less-ordered regions of cellulose are entrapped within the more crystalline regions; therefore, the rate of hydrolysis is limited by that of the crystallites. Furthermore, the observed increase in the average size of the crystallites during the treatment indicated a heterogeneous hydrolysis where only the lower molecular mass fractions are dissolved in subcritical water. Furthermore, the presence of cellulose II in the cellulose residue treated in near- and supercritical water was confirmed by XRS and NMR, which indicates either the homogeneous swelling of cellulose during the treatment, or the instantaneous adsorption of regenerated cellulose after cooling down the product (Tolonen et al. 2013).

The effect of catalysts on SCWT of MCC has also been investigated. Deguchi et al. (2008) reported that the presence of sulfuric acid in subcritical water led to a decrease to some extent in the crystalline-to-amorphous and dissolution temperature of MCC. However, a rapid corrosion phenomenon was observed at the higher temperatures and higher acid concentration. The addition of potassium carbonate as a base catalyst to MCC in subcritical water was analyzed by on-line gas chromatography and carbon balance (Kumar and Gupta, 2008). The results showed an increase in the formation of gaseous products along with the dark coloration of the liquid product fraction, which indicates that the presence of a base catalyst may promote the gasification and liquefaction reactions of carbohydrates in subcritical water.

Several alternative production pathways to SCWT have been developed for producing water-soluble cello-oligosaccharides (presented in Section 2.2.3.). However, producing water-insoluble cellulose polymers with low DP has received significantly less attention. Ball-milling, associated with acid catalysts, was shown able to break the crystalline structure of cellulose and produce low DP cellulose polymers. The combination of ball-milling and non-thermal atmospheric plasma treatment has been applied to MCC and resulted in the formation of low DP cellulose polymers, including both water-soluble and water-insoluble DP ranges, with high reported yield and low amount of degradation products (Benoit et al. 2012). The enzymatic depolymerization of microcrystalline cellulose in ionic liquids has been one other recent method proposed for producing low DP cellulose oligomers (Wahlstrom et al. 2012).

However, despite the high energy and high quality equipment requirements, short reaction times as well as the sole use of water are two strong advantages in favor of SCWT for producing short cellulose polymers. Therefore, SCWT is today considered a potentially viable method for producing water-soluble COSs and low DP cellulose II.

2.4. OBJECTIVES

The previous Section showed that the kinetics and products formation from microcrystalline cellulose in supercritical water has been the focus of a significant number of research publications in the last two decades. In addition, ultrafiltration has been considered a simple and potentially efficient method for isolating carbohydrate oligomers from liquid organic mixtures. However, to the author's knowledge only a few studies have considered the combination of SCWT and ultrafiltration as a novel way of producing purified cello-oligosaccharide mixtures. In addition, the literature shows that in parallel with water-soluble COSs low DP cellulose II can be easily obtained and isolated after precipitation and separation.

This thesis aims to provide an experimental basis for producing cello-oligosaccharides from microcrystalline cellulose at a daily gram scale using a combination of supercritical water and ultrafiltration methods.

The following sections develop the experimental work performed in this thesis. Section 3 describes the materials and experimental methods which were used, including sample production and characterization methods. Section 4 presents and describes the main experimental results and discusses both their more theoretical and more practical implications. In addition, Section 4 evaluates the feasibility of a cello-oligosaccharides production process using SCWT. Section 5 provides the main conclusions of this work, as well as directions for future research related to SCWT for cello-oligosaccharides production.

3. MATERIALS AND METHODS

3.1. MATERIALS

3.1.1. MICROCRYSTALLINE CELLULOSE

The microcrystalline cellulose (MCC) used in this thesis was purchased from Merck (Reference 1.02330.0500). The use of similar raw material has been reported for studying cellulose degradation in supercritical water; its crystallinity was 52 % when measured using wide-angle x-ray scattering (WAXS) (Tolonen et al. 2011). Its indicative particle size was < 20 μm and its measured dry matter content was 97 %. The MCC was used as received and was considered as pure cellulose, therefore with an average molecular formula $(C_6H_{10}O_5)_n$.

The size-exclusion chromatography (SEC, further described in Section 3.2.4.) analysis of the MCC gave a number-average molecular mass (M_n) of 12.8 kg/mol and a weight-average molecular mass (M_w) of 58.9 kg/mol, corresponding to a number average and mass average degree of polymerization of 79 and 363, respectively. The polydispersity index was 4.6. Therefore, the molecular mass distribution of the initial cellulosic raw material showed a relatively wide distribution of cellulose polymer chain lengths, as a result of acid hydrolysis and random depolymerization of natural cellulose Figure 9 shows the MMD of MCC.

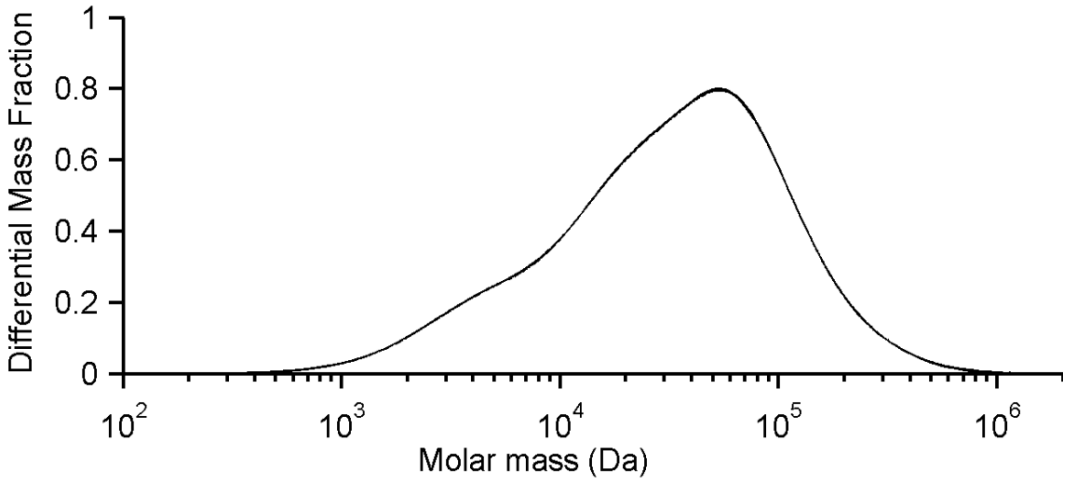

Figure 9. Molecular mass distribution of microcrystalline cellulose.

3.1.2. OLIGOMERS

Glucose and cello-oligosaccharides were used as reference compounds for calibrating the high-performance anion-exchange chromatography (HPAEC) apparatus and quantifying the peaks of the samples. Cellobiose was purchased from Fluka (Reference 22150), cellotriose, cellotetraose, cellopentaose and cellohexaose were purchased from Megazyme (References O-CTR, O-CTE, O-CPE, O-CHE). Cellobiose had a purity > 99 %, while cellotriose, cellotetraose and cellopentaose had purities > 95 %, and cellohexaose had a purity > 90 %.

3.1.3. FILTERS

Syringe filters were used in gravimetric analyses, for separating the solid fractions of the samples, and prior to all analyses of the liquid fractions. The filters were purchased from Pall (Pall Corporation, NY, US). For solid residue removal, syringe filters with 1 µm glass fiber membranes (Reference 4523T) with 25 mm diameter were used. For solid precipitate removal and for solids removal of the liquid fractions, 0.2 µm hydrophilic polypropylene syringe filter membranes with diameters of 13 and 25 mm were used (References 4554T and 4564T, respectively).

Flat, circular membrane filters were used for isolating the solid precipitate fraction from the samples. The membranes were purchased from Millipore (Reference S-Pak 0.2 µm). They had a nominative pore diameter of 0.2 µm and a diameter of 47 mm.

Three flat sheet hydrophilic polyamide membranes with respective molecular weight cut-off (MWCO) values of 270, 1000, and 3000 Da were used for filtering and purifying the cello-oligomers from the liquid product fractions. The membranes were purchased from Sterlitech (Sterlitech Corporation, Kent, US): Dow Filmtec model NF270 with a MWCO of 270 Da, GE Osmonics model UF GE with a MWCO of 1000 Da, and GE Osmonics model UF GK with a MWCO of 3000 Da. The membranes

were cut into circular pieces of diameter 62 mm in order to fit into the filtration cell (further described in Section 3.2.8.).

3.1.4. LIQUID CHEMICALS

Deionized water was used for the supercritical reactor system and for preparing the cellulose suspensions. Milli-Q water (Millipore Corporation, Billerica, US) was used for dilution and analytical analyses of the produced samples. Reagent-grade acetone (Reference 20066.300) and N,N-dimethylacetamide (Analysis-grade, reference 83636.350) were purchased from VWR (VWR International, France) used during the preparation of samples for size exclusion chromatography (SEC) and had purities higher than 99.9 % and 99.5 %, respectively.

3.2. METHODS

3.2.1. SUPERCRITICAL WATER REACTOR SYSTEM

The degradation of microcrystalline cellulose at high temperature and pressure was performed using a sub- and supercritical water reactor system. The system was designed and manufactured by Karlsruhe Institute of Technology, and data from this apparatus have already been reported (Tolonen et al. 2013). The following sections present the main characteristics and operational principles of the system.

3.2.1.1. REACTOR FEATURES

The core of the system was the reactor unit, comprised of a monobloc, stainless steel reactor unit having a fixed tubular reaction volume V of 389 µl (internal diameter 3 mm, length 55 mm), and two perpendicular T-shaped inputs and one perpendicular output. In addition to the physical reaction volume the reactor unit included three temperature sensor connections and an external heating system. Figure 10 shows the industrial design of the reactor.

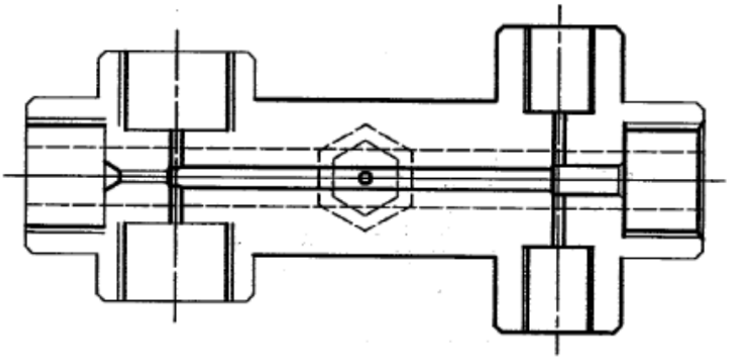

Figure 10. Design of the reactor.

In normal operation two streams were fed and mixed together at one end of the reactor, namely the cellulose suspension and the preheated water. The reaction took place as the heated cellulose suspension flowed inside the tubular reactor, until cold quenching water was fed at the other end of the reactor and stopped the reaction by rapidly mixing and cooling down the suspension. Therefore, the reactor was considered a plug flow reactor and the reaction time was determined by the residence time of the suspension inside the reactor at treatment temperature. In addition, heating elements on the outer side of the reactor compensated for heat losses to the atmosphere.

Assuming the mixing of a water stream and a suspension stream to be a total and instantaneous phenomenon, the residence time is a function of the reaction volume and two operational parameters: the density and the mass flow of the cellulose suspension in the reactor. All the reactions were performed at low suspension consistency (0.5 wt%); therefore, the density of the suspension at reaction temperature ρ and pressure was approximated as the density of pure water at the same reaction temperature and pressure. The mass flow ṁ was adjusted by the operating parameters of the high pressure pumps (further described in Section 3.2.1.3.). Consequently, the reaction time τ was calculated using the Equation 2.

$$\tau = \frac{V \times \rho}{\dot{m}} \qquad (2)$$

3.2.1.2. REACTOR SETUP

The three streams fed to the reactor originated from two tanks kept at room temperature, namely the water tank and the cellulose tank. The water tank was filled with deionized water and provided water for both heating and quenching streams. The cellulose tank was filled with MCC suspension in deionized water, and was kept in constant agitation using an external circulation flow as well as a stirring system inside the tank.

Downstream of the reactor the suspension was further cooled down by flowing through a cooling jacket (tubular liquid-to-liquid heat exchanger), which decreased the temperature of the suspension below 60 °C. The suspension then flowed through a manual back-pressure regulator that depressurized the suspension into atmospheric pressure before being collected in the sampling area. The back-pressure regulator was the pressure control equipment for the whole pressurized circuit.

3.2.1.3. HIGH-PRESSURE PUMPS

Supercritical pressures inside the system were reached using a block of three high-pressure diaphragm metering pumps (LEWA model EK3, LEWA Gmbh, Leonberg, Germany). The pump strokes were connected to the same motor, which had a global frequency regulation system and individual stroke length adjustment handwheels. Therefore, the volumetric flow of each pump could be adjusted separately.

The residence time of the treatment is a critical parameter for the degradation of microcrystalline cellulose in sub- and supercritical water. It can be adjusted according to Equation 2 and requires the knowledge of the mass flows delivered by the high-pressure pumps. Therefore, a preliminary series of experiments was conducted in order to determine the mass flows for each of the three pumps as a function of their two operating parameters, namely the stroke frequency and the individual stroke lengths. Combinations of five frequencies and three stroke lengths

were run with deionized water for each of the three pumps. Three polynomial functions were extracted from the obtained experimental mass flows using the Curve Fitting Toolbox of MATLAB. Figure 11 shows an example of curve fit for the cellulose suspension pump. The curve fits for the three high-pressure pumps can be found in Appendix B.

The three pump model functions were used for predicting and adjusting the mass flows to the desired operating parameters of the system. The model proved to be reliable, with measured mass flows generally within 5 % relative error when compared to the projected values. A graph presenting the mass flow projections can be found in Appendix B.

3.2.1.4. THERMODYNAMICS

In addition to the mass flows of the pumps, characterizing the SCWT system was needed prior to producing the samples in order to be able to operate at the desired reaction conditions. Four main hypotheses and simplifications allowed building a simple mass and energy balance. Given the low consistencies the cellulose suspension flows were assumed to have the same properties as pure water under the same conditions. The external heating elements of the reactor only compensated for heat losses and did not provide additional energy to the system. No other heat losses were considered than the heat losses compensated by the reactor heating elements. The Reynolds number for a similar reactor under similar operating conditions was calculated by Aksoy (2011) and indicated turbulent flows, which led to assuming the mixing of two flows inside the reactor to be complete and instantaneous. Therefore, the reactor system was considered operating under ideal conditions both regarding the mass and energy balance.

The density and the enthalpy of water at various temperatures and at 250 bar were retrieved from the NIST Webbook database (Lemmon et al.) and interpolated into polynomial functions using the Curve Fitting Toolbox of MATLAB. The mass flow and specific enthalpy of a fluid stream resulting from the mixing of two streams using their respective mass flows was calculated according to Equation 3 and 4,

respectively. The consistency c of a suspension stream after mixing with a water stream was calculated using Equation 5.

$$\dot{m}_{1+2} = \dot{m}_1 + \dot{m}_2 \quad (3)$$

$$h_{1+2} = \frac{\dot{m}_1 \times h_1 + \dot{m}_2 \times h_2}{\dot{m}_1 + \dot{m}_2} \quad (4)$$

$$c_{1+2} = c_1 \times \frac{\dot{m}_1}{\dot{m}_1 + \dot{m}_2} \quad (5)$$

The prediction of the required adjustment parameters (preheater temperature, stroke frequency, individual stroke length) to operate at desired operating parameters (treatment temperature and consistency, residence time, consistency) was achieved by combining Equation 2, Equation 3, Equation 4, and Equation 5 together and using the Solver function in Microsoft Excel.

In addition to the mass and energy balance the determination of the heating power of the water preheater was required in order to assess the electric consumption of the system. Assuming a steady state with no heat losses, the required preheater power was estimated using preheater mass flow and tabulated water enthalpy values according to Equation 6.

$$P_{preheater} = \dot{m} \times \frac{(h_{water,(420°C)} - (h_{water,(20°C)})}{\eta} \quad (6)$$

Assuming a steady state and tubular reactor geometry, the heat losses in the reactor area were estimated using the reactor dimensions, differential temperature and thermal conductivity of the reactor material according to Equation 7.

$$P_{losses} = \dot{m} \times 2\pi \times L_{reactor} \times k_{steel} \frac{(T_{reaction} - T_{atm})}{\ln(\frac{r_{ext}}{r_{int}})} \quad (7)$$

In addition, the shaft power required by the pumps to deliver the required mass flows at selected operating pressure were estimated using fluid mass flow, differential pressure and estimated pump efficiency according to Equation 8.

$$P_{pump} = \dot{m} \times \frac{P_{system} - P_{atm}}{\eta} \quad (8)$$

3.2.1.5. CONTROL AND AUTOMATION

The system had five temperature indicators, including one temperature control regulating the heating power of the preheater and one temperature control to adjust the reactor temperature. The reaction was kept at nearly constant temperature inside the reactor using an outside wall heating system, in order to compensate for heat losses. Therefore, the operating parameters for the SCWT system were the temperatures of both heating water and reactor external surface, the pressure of the back-pressure regulator, the frequency of the pump group and the three individual stroke lengths of the high-pressure pumps. Changing the frequency and the individual lengths allowed adjusting each of the three flows to the reactor (cellulose suspension, heating water, quenching water), and therefore the reaction time and temperatures (temperature inside the reactor, temperature after quenching). Figure 11 shows a schematic representation of the system.

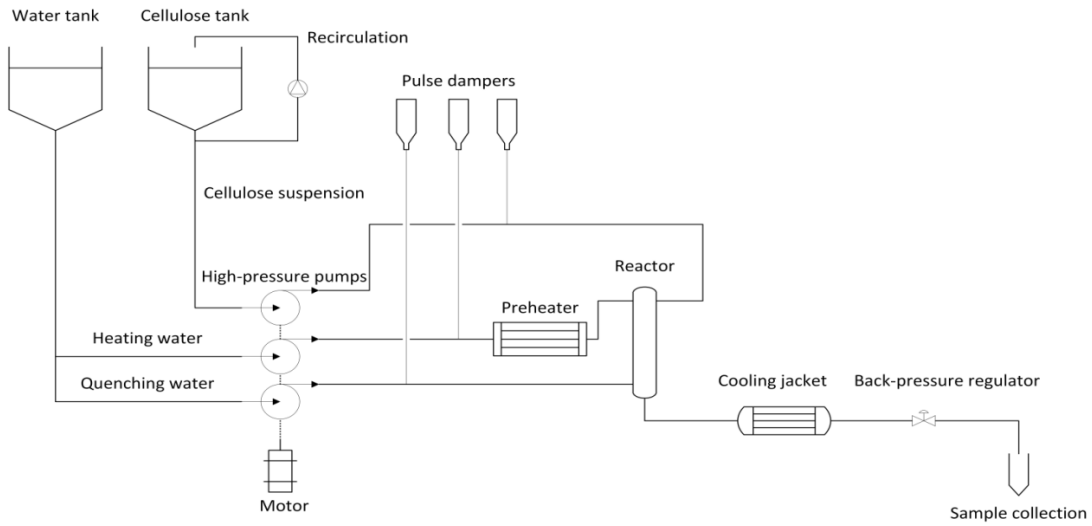

Figure 11. Overall scheme of the reactor system.

3.2.2. EXPERIMENTAL PROCEDURE

The experiments included producing 19 series of samples (at different combinations of reaction temperature and reaction time), in order to obtain results within an

extensive range of operating parameters, both in subcritical and supercritical water. In order to allow comparing the results with previous studies and due to a lack of regulation sensitivity as well as a limited range of available operating pressures the reaction pressure was chosen to be set at 250 bar for all the samples. The procedure for operating the SCWT system can be found in Appendix B.

The samples were treated in the temperature range from 320 °C to 390 °C and at residence times from 0.1 s to 0.8 s. Due to physical limitations of the system the lowest residence times could only be reached at the highest reaction temperatures. The density of water decreases significantly under near- and supercritical conditions, which allowed slightly decreasing the lower residence time under supercritical temperatures. The detailed experimental plan and corresponding operating conditions can be found in Appendix E, as well as some of the properties of water at corresponding treatment temperature which are presented in Appendix A. In order to understand the mechanism of microcrystalline cellulose degradation a series of analyses was performed on the products of each of the 19 studied conditions. However, after production one sample was found to be repeatedly inconsistent with the others, presumably due to a malfunction in initial filtration. Therefore, only 18 samples are included in the results presented in Section 4.

The fractionation scheme that followed the sample collection applied for each of the 18 produced series of samples is depicted in Figure 12. Once the desired operating conditions was reached the product flow was either directly collected into a 40 ml centrifuge tube, or immediately filtered through a 1 µm syringe filter. The liquid filtrate was collected into a centrifuge tube for further analyses. The latter operation was performed twice. Each sample was collected in duplicate; therefore, each series of sample consisted in collecting six centrifuge tubes, of which four were immediately filtered. Since collecting the samples was a long operation at high residence times the sampling operation was considered valid only if the displayed reaction temperature fluctuated by a maximum of two degrees between the first sample and the last sample.

The solid residue fraction was collected immediately after sampling by centrifuge using an Eppendorf 5804 R apparatus with a capacity of six 50 ml tubes for 20 min at 10,000 rpm (equivalent relative centrifugal force 12850 g). The supernatant liquid phase was removed and the sediment solid fraction was collected for further analysis. The other collected samples were stored at 5 °C for further analysis. The solid precipitate fraction was collected after five days (120 hours) of settling at a temperature of 5 °C. In most of the samples a precipitation phenomenon was observed, which occurred after a short settling time. The samples were filtrated through a 0.2 µm membrane filter using a 250 ml Sartorius filtration funnel. The solid residue was collected from the surface of the membrane filter for further analysis. The overall analysis scheme can be found in Appendix C.

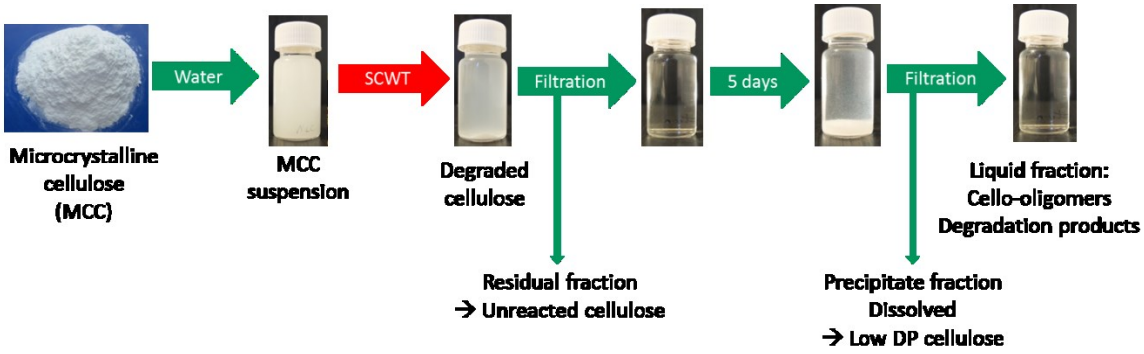

Figure 12. Sample fractionation procedure.

3.2.3. CONVERSION OF CELLULOSE

Published literature showed that microcrystalline cellulose undergoes degradation in water under sub- and supercritical conditions. The extent to which the initial cellulose suspension has been degraded at specific reaction time and temperature must be identified first. Therefore, the cellulose degree of conversion, defined as one minus the ratio between the consistency of the cellulose suspension after treatment and the consistency of the initial cellulose suspension, was used as a general indicator for the severity of the treatment, and served as a basis for characterization of the reaction products. The degree of conversion X was calculated from the cellulose consistency before and after reaction according to Equation 9.

$$X\ (\%) = 1 - \frac{[C]}{[C]_0} \quad (9)$$

The knowledge of the degree of conversion allows making assumptions on the kinetics of cellulose degradation. Assuming that the reaction rate k is only a function of the cellulose consistency in the suspension, a first-order kinetic model can be developed and verified against the experimental values obtained for the cellulose conversion according to Equation 10. Validating the kinetic model allows determining the first order kinetic constant of the reaction, calculated by plotting experimental data according to Equation 11.

$$\frac{d[C]}{dt} = k \times [C] \quad (10)$$

$$\mathrm{k} = -\frac{\ln(1-\mathrm{X})}{\tau} \quad (11)$$

The values of the kinetic constants of the reaction, as well as the assumption that the reaction of cellulose degradation follows an Arrhenius-type equation, allows calculating the activation energy of the reaction at different reaction temperatures, as well as the pre-exponential factor, according to Equation 12.

$$\mathrm{k} = \mathrm{A}\, e^{-\frac{E_a}{\mathrm{RT}}} \quad (12)$$

The following sections describe the analytical methods used for characterizing the product fractions.

3.2.4. TOC

Total organic carbon (TOC) measurements were performed in order to quantify the organic components in the sample and served as a basis for the mass balance of the products. TOC measurements were performed using a Shimadzu TOC-V CPH apparatus.

The samples were filtered through a 0.2 µm syringe filters and diluted with purified water to a ratio of 1:1 in order to lower the maximum theoretical carbon content below the upper limit of the linear response range of the apparatus.

The apparatus gave the total carbon and the inorganic carbon contents of the sample. The total organic carbon was obtained by difference. Assuming pure cellulose as the raw material of the samples and assuming that the average chemical formula remained unchanged after treatment (no gas removal, average chemical composition of the samples $C_6H_{10}O_5$), the total organics (TO) content of the samples were calculated using the Equation 13.

$$\mathrm{TO\ (mg/l)} = \mathrm{TOC\ (mg/l)} \times \frac{162}{72} \tag{13}$$

3.2.5. HPAEC-PAD

High performance anion-exchange chromatography with pulsed amperometric detection (HPAEC-PAD) was used in order to quantify the water-soluble cello-oligomers in the product samples, using a Dionex ICS-3000 apparatus (Dionex, Sunnyvale, USA) equipped with a Dionex CarboPac PA100 column. Calibration curves were obtained from standard glucose and cello-oligomer compounds with DP 2 to 5 using solutions with concentrations ranging from 2 to 50 mg/l. The linear behavior of the curves suggested that those concentrations were within the linear response range of the apparatus. Assuming that the response range remained valid for higher DP oligomers and due to the lack of standards available for cello-oligomers with DPs higher than 6 the obtained calibration curves were then extrapolated to DP 10 according to a method already described by Yun and Wu (2009). The calibration curves obtained from standard compounds as well as the extrapolated curves and their fit can be found in Appendix D.

3.2.6. SEC

Size exclusion chromatography (SEC), also referred to as gel permeation chromatography (GPC), is a chromatographic analytical method that provides the

molecular mass distribution of a polymer sample. It comprises a column packed with specific porous material through which a dissolved polymer is eluted. As a result the elution time is a function of the size of the polymer, the larger molecules eluting more rapidly than the smaller molecules. SEC was performed using a Dionex Ultimate 3000 system calibrated using pullulan standards. The solid product fractions of the samples were analyzed in order to determine their molecular mass distributions and therefore to analyze the effect on reaction conditions on the initial microcrystalline cellulose. The samples were prepared according to the following procedure: they were successively activated in Millipore water, acetone, DMAc, and saturated DMAc/LiCl (90 g/l). Each solvent exchange operation was performed with three successive steps of centrifugation and solvent replacement. Once dissolved in DMAc/LiCl the samples were diluted using DMAc to reach a desired approximate dissolved sample concentration of 1.0 mg/ml, stirred thoroughly for 10 minutes, filtered through a 0.2 µm syringe membrane filter into a vial for analysis. Each sample was analyzed in duplicate (two 100 µl injections).

Formatting of the SEC data was done according to the following procedure. The apparatus returned the differential molecular mass fraction as a function of the logarithm of the sample molecular mass. Decimal scale was found more relevant in the case of low molecular mass samples; therefore, the curves were integrated (using the trapeze method), converted to decimal scale, derived, and normalized. Number- and weight-average degrees of polymerization as well as polydispersity index were calculated from the resulting data according to the following Equation 14, Equation 15, and Equation 16, respectively (Vega et al. 2004).

$$M_n = \frac{\sum M_i N_i}{\sum N_i} \quad (14)$$

$$M_w = \frac{\sum M_i^2 N_i}{\sum M_i N_i} \quad (15)$$

$$PDI = \frac{M_w}{M_n} \quad (16)$$

3.2.7. MEMBRANE FILTRATION

Membrane filtration was performed using an Amicon 8200 batch stirred cell. The filtration system was maintained at 5 bar pressure inside the cell using pressurized nitrogen. The membranes were cut at the cell size from the purchased flat sheets and soaked in deionized water overnight before use. Two experiments were conducted: simple filtration, and continuous filtration. In simple filtration 150 ml of sample was inserted into the cell and filtrated up to a residual volume of about 30 ml. In continuous filtration about 10 ml of the retentate obtained in simple filtration were inserted into the cell. Approximately 500 ml of deionized water was added in successive steps into the cell and filtrated up to a retentate volume of about 10 ml. Both filtration methods were tested using the three different membranes (presented in Section 3.1.3.). The initial sample, retentate, diluted retentate, and permeate fractions were then analyzed by HPAEC-PAD for oligomer content determination (according to the procedure described in Section 3.2.5.).

3.2.8. TECHNO-ECONOMIC ANALYSIS

In order to assess the feasibility of the SCWT of cellulose a simple techno-economic analysis was conducted. A process concept for producing cello-oligosaccharides was developed based on the supercritical water system, operating conditions and results presented in this thesis (described in Section 3.2.1. and further described in Section 4.2 and section 4.4) as well as reported data from literature (Huebner et al. 1978, Zhang & Lynd 2003).

The process considered consisted in six unit operations: SWCT, first solids removal, purification, second solids removals, fractionation, and drying. In this process a cellulose suspension is mixed with preheated water at near-critical or supercritical conditions into an isothermal reactor (as described in Section 3.2.1). The suspension is quenched with cold water, further cooled down and relieved to atmospheric pressure. The next step removes the residual solid fraction (e.g., by simple microporous polymer membrane filtration). The obtained liquid fraction is purified from low molecular mass degradation products and salts through a pressurized

ultrafiltration cell unit similar to that presented in Section 3.2.7. The filtration also allows concentrating the product, resulting in a rapid precipitation of the higher DP oligomers, which can be removed in a second filtration step. The purified retentate fraction is fractionated in a chromatography column packed with ion-exchange resin similar to that already presented and successfully applied in the literature, where individual oligomer fractions are collected up to DP 6 (depending on the separation power of the column), and a mixture containing higher cello-oligomers. The final step consists in drying the previously obtained, individual fractions into powder using a spray-drying system.

The main design parameters include the electrical power of the pump motor and the preheater, the size and volume of the reactor, the solid-liquid separation (filtration) technology, the area of the ultrafiltration membrane, the size and volume of the column, and the size and flows of the spray-dryer. In addition to the design parameters, several operating parameters can be adjusted during the system operation, which have an influence on the product yield and composition, as well as the overall operating costs of the plant. The operating parameters include the reaction pressure, temperature and residence time (determined by the pump flows), as well as the nature of the cellulosic raw material and its consistency in the suspension. Other operating parameters are the characteristics of the ultrafiltration membrane (MWCO), the nature of the ion-exchange resin, and the flows and temperature for the spray-dryer.

The details of the costs and production streams can be found in Appendix F. However, these calculations must be considered carefully as they are only based on simplified thermodynamic concepts, simplified process requirements, and indicative equipment prices publicly available on the Internet.

4. RESULTS AND DISCUSSION

The following section presents the main experimental results obtained with the materials, methods and experimental scheme presented in Section 3. Section 4.1 studies the degradation of microcrystalline cellulose in near- and supercritical water. Section 4.2 investigates the nature, yield and composition of the solid and liquid products of the reaction. Section 4.3 focuses on the molecular mass distribution of the cellulosic product fractions. Section 4.4 describes the efficiency of membrane ultrafiltration for purifying the water-soluble cello-oligosaccharides formed during the SCWT of MCC. Section 4.5 presents a production scheme for cello-oligosaccharides using SWT as well as a cost structure analysis of such system.

4.1. CELLULOSE DEGRADATION

Under most of the investigated treatment temperature and residence time the freshly-produced, unfiltered samples showed a white, cloudy coloration, indicating that some undissolved cellulose was present as a suspension in the product. The degree of conversion, defined as the amount of unreacted cellulose related to the overall product contents (on product TOC basis), is shown in Figure 13.

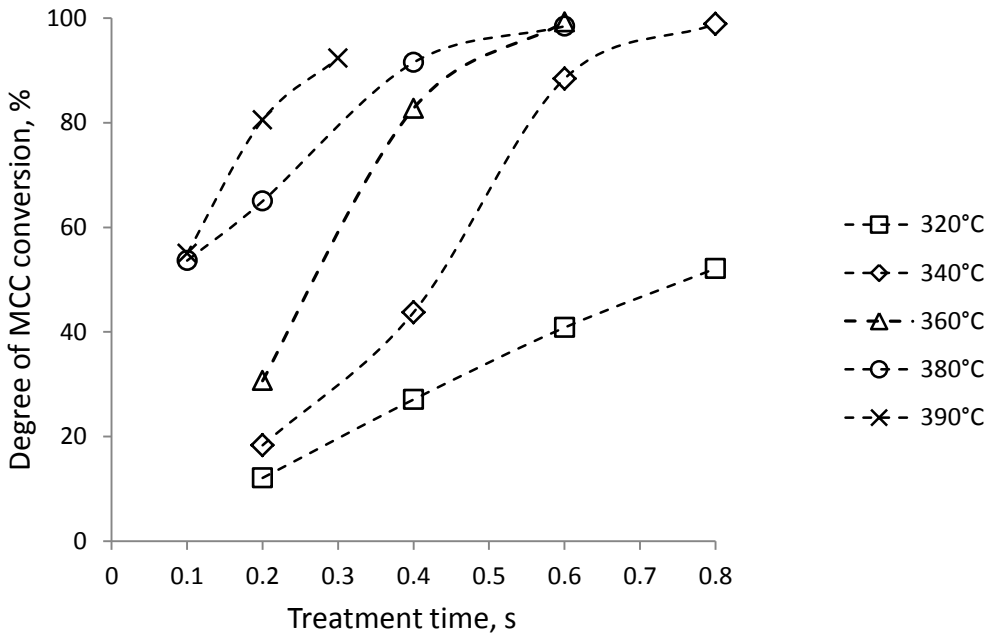

Figure 13. Conversion of cellulose vs. treatment time.

The conversion of cellulose increased with increased reaction time, ranging from 12 % (0.2 s at 320 C), to nearly 99 % (0.8 s at 340 C, 0.6 s at 360 C and 380 C). In addition, the degree of conversion at a given treatment time was higher at higher temperature. Cellulose conversion as a function of residence time seems to follow a rather linear trend where the conversion rate was significantly lower. A similar trend for the evolution in the degree of conversion with increased temperature and time has been reported for treatment in subcritical water by Yu and Wu (2010).

Even under severe conditions residual cellulose was found in every product, which can be explained by the slower rate of conversion as the consistency of the initial cellulose decreased. In addition, the latency of a few seconds between the time of sample production and the collection of its solid fraction can explain that residual cellulose was found in samples even at high treatment severity. Yu and Wu (2009) observed that the precipitation of cellulose immediately starts after cooling down. Further analysis of the solid residue fraction would reveal the allomorphic nature of the residue. The presence of cellulose II in residue would either indicate the swelling of microcrystalline cellulose in scH_2O or the adsorption of regenerated cellulose II on the surface of the cellulose I residue, as previously reported in the literature (Tolonen et al. 2013). However, these results show that cellulose conversion is a good indicator for the degree of advancement in the hydrolysis of MCC. Therefore, the degree of conversion of microcrystalline cellulose is used for characterizing the product formation in Section 4.2.

The degradation of microcrystalline cellulose in supercritical water has been repeatedly characterized in the literature assuming a first-order reaction model and an Arrhenius-type reaction. A good fit of the experimental values as already presented in Section 2.3.3 and reported in several papers (Sasaki et al. 2000, Tolonen et al. 2011, Cantero et al. 2013). A shirinking grain model was also developed by Sasaki et al. (2004) based on microscopic observations of the size of the crystallites, but this model is not considered in this study. Figure 14 shows the reaction rate of the experiments conducted in this present study, assuming a Arrhenius-type first- order reaction.

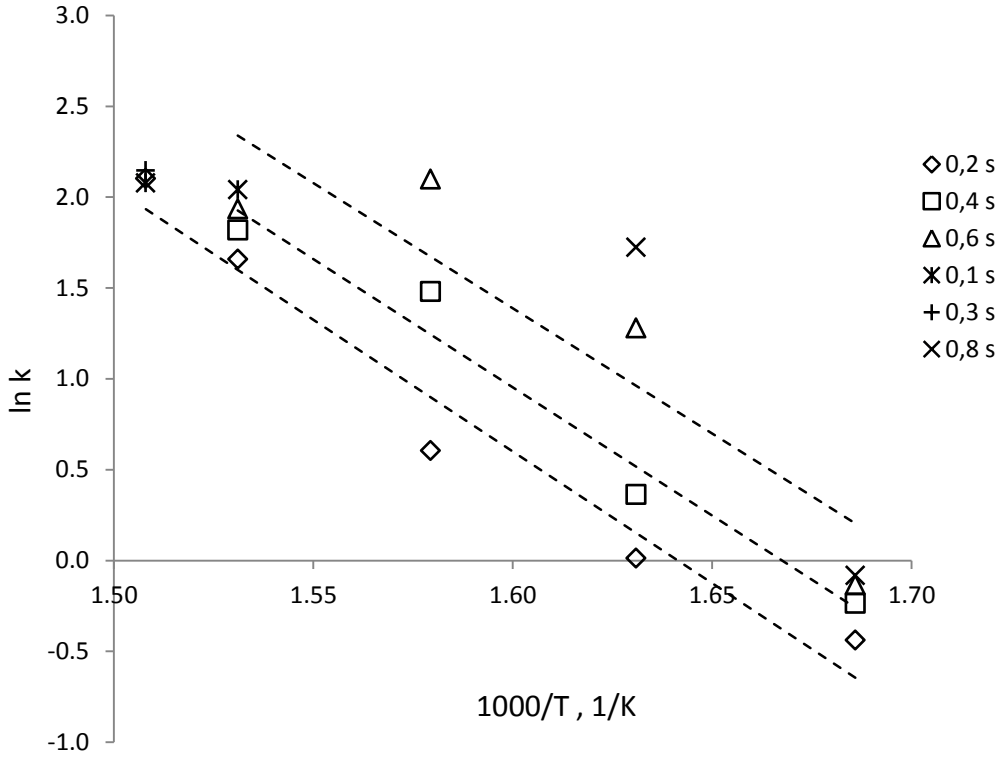

Figure 14. Arrhenius plot of first-order cellulose decomposition rate constants.

The previously reported results for the decomposition rate constants showed a relatively good accordance with the Arrhenius-type first-order kinetic model. The values obtained during the present experiments showed a rather linear distribution, which would confirm the hypothesis of a first-order reaction. However, a significant scattering was observed for the values obtained at different reaction times. Moreover, Sasaki et al. (2000) previously reported an increase in the hydrolysis rate for temperatures above the critical point of water, which has not been observed in the present data.

Assuming a first order Arrhenius-type reaction the average obtained activation energy for the decomposition of cellulose is 117 kJ/mol (114 kJ/mol, 117 kJ/mol and 120 kJ/mol for reaction times of 0.2 s, 0.4 s, and 0.6 s, respectively). These values are lower than the activation energy of 146 kJ/mol and 154 kJ/mol for cellulose hydrolysis reported by Sasaki et al. (2004) and Cantero et al. (2013), and considerably lower than the activation energy of 225 kJ/mol obtained in subcritical water treatment by Tolonen et al. 2011.

One reason for the limited fit of the experimental data with other results from literature is that that the treatments were performed at short residence times and high reaction temperatures near the limit of the operating range of the system. Although the mass flows matched the projected model with good accuracy the design of the reactor does not guarantee a perfectly isothermal reaction profile. In addition, slight imprecisions in the reaction temperature can lead to significant changes in the conditions inside the reactor, impacting the reaction parameters especially at higher treatment temperature and shorter residence time. In addition, and despite the turbulent flow regime inside the reactor, the assumption that the mixing between preheated water and cellulose suspension is perfect and instantaneous has not been demonstrated at such short residence times. A more accurate control of the temperature profile inside the reactor such as the reactor used by Cantero et al. (2013), as well as additional experiments under milder conditions would give more insight to the observed scattering of the obtained decomposition rate constants.

4.2. PRODUCT COMPOSITION

The product quantification methods (presented in Sections 3.2.2 - 3.2.5) allowed identifying and quantifying four product fractions, in accordance with previous results from literature: solid residue, solid precipitate, water-soluble cello-oligomers, and water-soluble degradation products. The numerical values can be found in Appendix E. Figure 15 shows the evolution of the formation of each product fraction as a function of the cellulose degree of conversion. For a more comprehensive understanding of the direct influence of temperature and residence time on the product composition of the samples the mass balance of the sample fractions are presented in Appendix E.

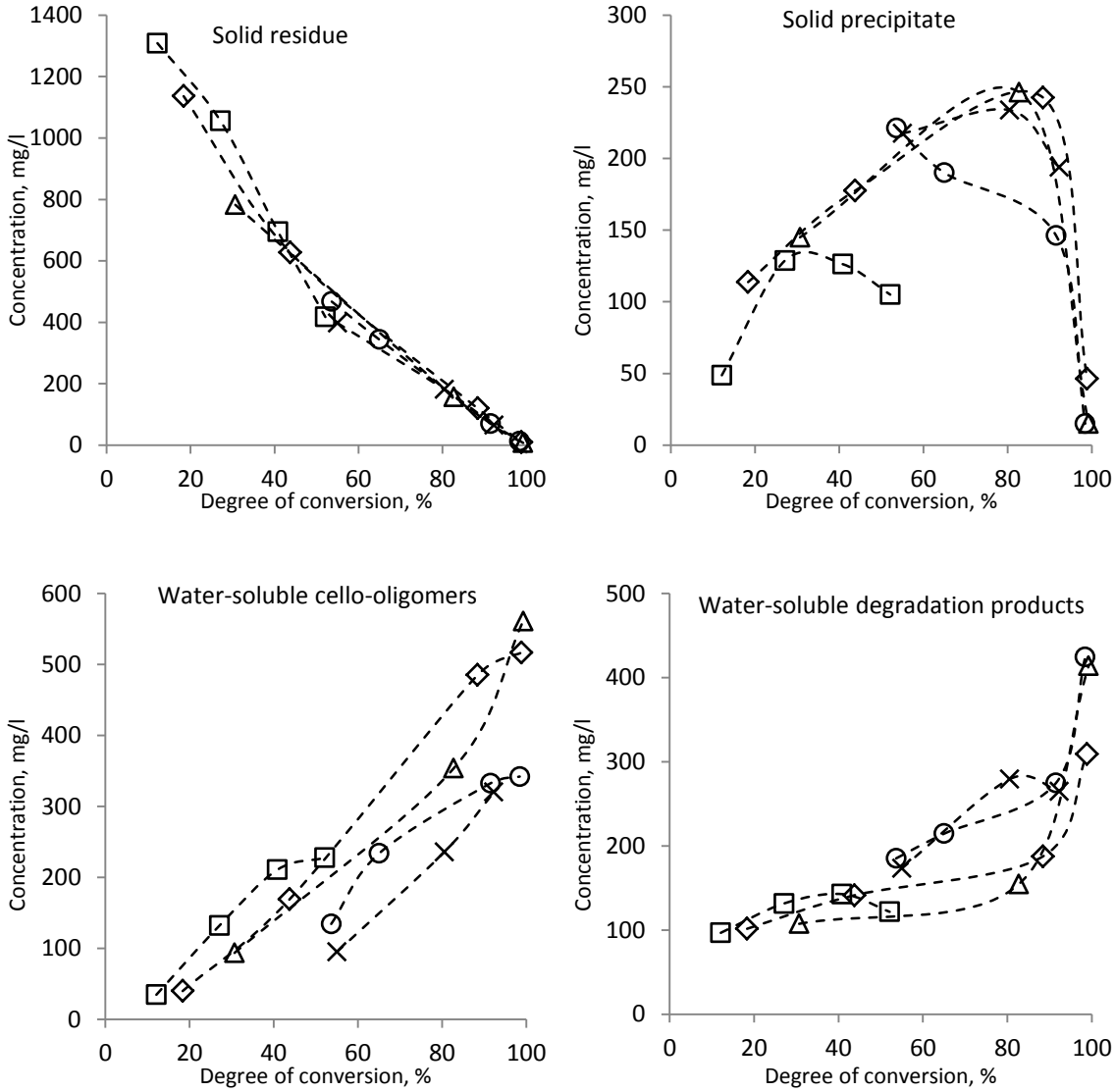

Figure 15. Composition of the four product fractions vs. cellulose conversion.

Legend: □ 320 °C; ◊ 340 °C; Δ 360 °C; O 380 °C; X 390 °C

The consistency of the solid residue fraction in the product fraction showed a linear decrease with increasing cellulose conversion rate. This observation is consistent with the assumption that the solid residue is composed of residual, unreacted cellulose.

With the exception of values obtained at 320 °C, the amount of precipitate increased with the degree of conversion and following the same pattern independently of the treatment temperature, and reached maximum consistency levels of about 250 mg/l or 25 % at conversion values around 85 %. The precipitate

consistency dropped rapidly at higher conversion degrees to values near zero at maximum cellulose conversion. At 320 °C the observed evolution for the formation of cellulose precipitate was different, with similar consistencies at low cellulose conversion levels but a decrease in precipitate formation at higher residence times.

The formation of water-soluble COSs increased with increasing cellulose degradation, with maximum levels of about 550 mg/l or 60 % reached at full cellulose conversion at 340 and 360 °C. This increase followed similar trends at the various studied reaction temperatures, although the yield of cello-oligosaccharide was significantly higher for lower temperatures at similar conversion rates. Under supercritical temperatures the maximum cello-oligosaccharides formation was about 270 mg/l. The temperature dependency for the water-soluble COSs formation can indicate that the rate of further degradation into other water-soluble products is increased at higher temperatures; therefore, lower treatment temperatures stabilize the COSs against further conversion and lead to higher yields.

The water-soluble degradation products fraction represents the amount of dissolved compounds that have not been identified as glucose or cello-oligosaccharides by anion-exchange chromatography. These products are formed via dehydration and retro-aldol fragmentation of mono- and polysaccharides, and several publications have already investigated the chemical nature of these non-cellulosic, water-soluble degradation products (Sasaki et al. 1998, Ehara and Saka 2002, Cantero et al. 2013). The formation of these products increased nearly linearly with increasing cellulose conversion up to concentrations about 400 mg/l or 50 % at conversion levels around 90 %. Above 90 % conversion these compounds were obtained in even larger quantities, reaching nearly 950 mg/l at full cellulose conversion (360 °C, 0.6 s). As for cello-oligosaccharides, the formation of degradation products was higher at 320 °C than at the other studied temperatures at similar cellulose conversion rates.

As far as the formation of solid precipitate the observed maximum at 85 % cellulose conversion supports the results of previous experimental studies, which suggested that glucose and cello-oligomers undergo further degradation in near-critical or supercritical water treatment, including dehydration or fragmentation reactions (Ehara and Saka 2002). At low cellulose conversion the depolymerization rate is higher than that of the degradation; therefore, the amount of formed precipitate increases. However, at nearly complete cellulose conversion the rate of the hydrolysis decreases and most of the formed precipitate is further degraded into products, which are soluble in ambient water.

To the author's knowledge the pattern of the precipitate formation with increasing cellulose conversion has not been reported in literature. Assuming a two-step mechanism, the concentration of precipitate as a function of cellulose conversion X can be expressed using Equation 17. The equation parameters are the apparent initial cellulose concentration C_0 as well as the rate constants of the first and second reaction k_1 and k_2, where k_1 is the rate constant of precipitate formation and k_2 is that of precipitate degradation.

$$P(X) = C_0 \times \frac{k_1}{k_2 - k_1} \times \left(e^{-k_1(100-X)} - e^{-k_2(100-X)}\right) \quad (17)$$

Figure 16 shows a curve fit obtained assuming a precipitate formation mechanism driven by two consecutive mechanisms using Equation 17 and the least-square method.

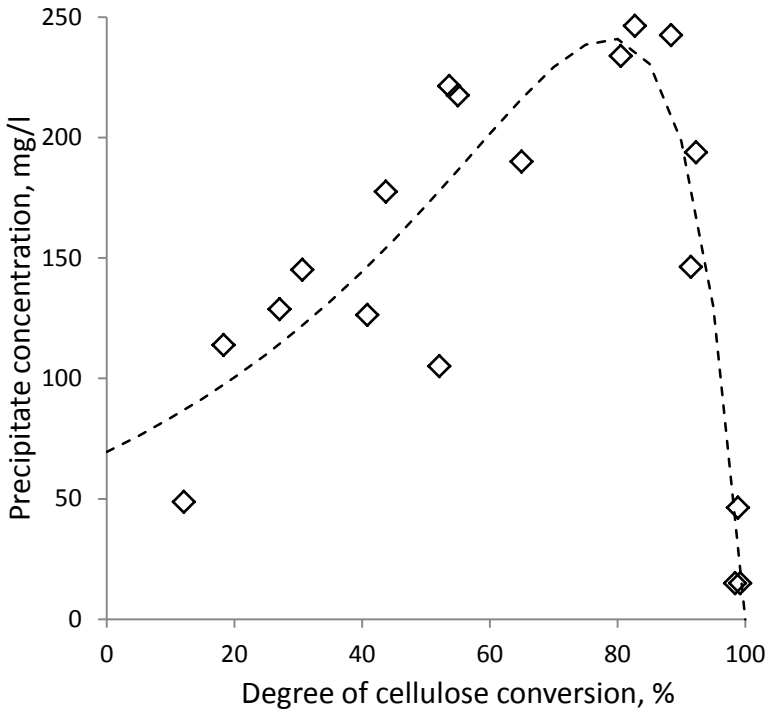

Figure 16. Model fit for precipitate formation.

The fit with the experimental values obtained in this study is relatively good and the observed pattern clearly shows a two-step mechanism of initial formation followed by faster degradation at increased cellulose conversion. However, it should be noted that the utility of this model is mainly limited to practical uses and does not directly describe the kinetics of precipitate formation. The model equation uses cellulose conversion X as a parameter instead of the treatment time t needed in kinetic studies. Furthermore, the experimental conditions impose an initial precipitate concentration of zero at zero cellulose conversion. seems to be required in order to fit the model with lower conversion, where almost no precipitate is formed. Additional experiments performed at low cellulose degrees of conversion would be likely to bring additional insight about the pattern for precipitate formation at various degrees of conversion.

As far as the precipitate, cello-oligosaccharides and degradation products are concerned, at 320 °C the degradation mechanisms are similar to those at other temperatures but seem to happen at different rates. Near- and supercritical

temperatures favor the hydrolysis mechanism of cellulose, but the formation of degradation products is significantly affected by the reaction temperature as well.

4.3. MOLECULAR MASS DISTRIBUTION

While gravimetric analyses only allowed the determination of the product mass balance and developing kinetic models for the formation of solid fractions HPAEC combined with TOC provided information about the cellulosic and organic composition of the liquid fractions. HPAEC also allowed calculating the concentration of glucose and water-soluble cello-oligosaccharide with a DP range of 2 to 10. In addition, the molecular mass distributions of both the solid residue and the solid precipitate were obtained using SEC. Figure 17 shows the evolution of the DP_w of the solid residue and precipitate fractions as a function of cellulose conversion.

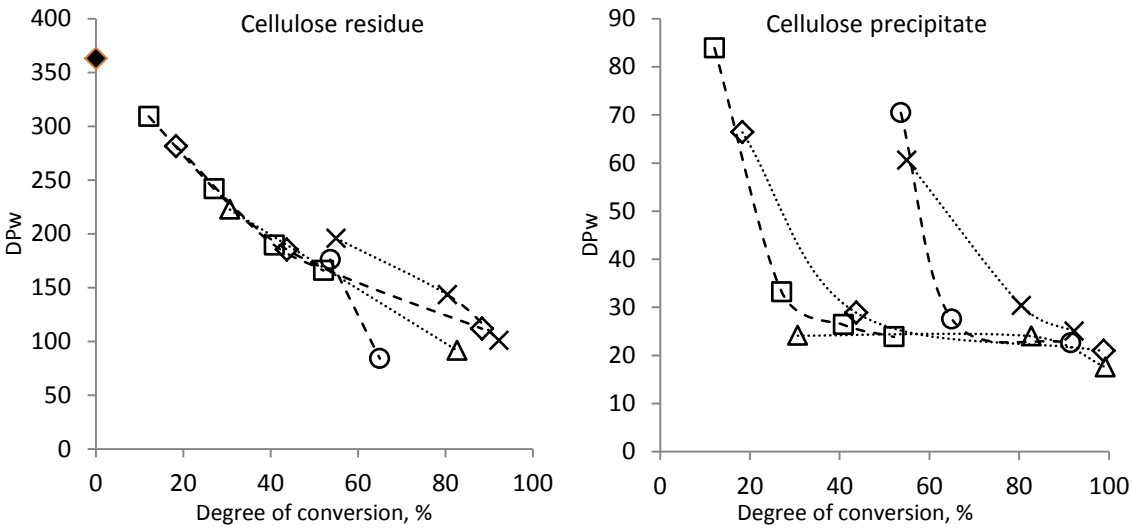

Figure 17. Weight-average degree of polymerization of the solid fractions.

Legend: ♦ MCC; □ 320 °C; ◊ 340 °C; Δ 360 °C; O 380 °C; X 390 °C

At sub- or nearcritical temperatures the residue fraction showed a relatively linear decrease in weight-average degree of polymerization, from the initial DP_w of unreacted MCC to values close to 100 at conversion rates around 90 %. Under supercritical conditions and especially at the highest temperature (390 °C) the trends remained similar but somewhat deviated from a totally linear decrease,

exhibiting slightly higher DP_ws. No residue fraction showed a DP_w below 85. In addition, at high cellulose conversion no significant residue fraction could be collected by centrifuge and analyzed by SEC. These results are consistent with the existence of a LODP in microcrystalline cellulose which was already observed in subcritical water treatment (Tolonen et al. 2011).

The DP_w of the precipitate showed a more peculiar evolution. At each temperature the value for the shorter residence time (lower conversion rate) was in the range from 55 to 85, while the following samples at higher cellulose conversion had their DP_w located around the value of 25 (minimum obtained value 18, maximum 33). No DP_w was recorded below 18, which can be explained as a result of the solubility of the low molecular mass cello-oligosaccharides even in ambient water. These values are consistent with previous molecular mass distribution analyses, where a DP range between 13 and 100 estimated by Ehara and Saka (2002) and a viscosity-average DP of 40 reported by Sasaki et al. (2003).

However, the sole knowledge of the evolution in the DP_ws is not sufficient to understand the cellulose depolymerization mechanism taking place in scH_2O. The evolution of the DP (on linear basis) and the Molecular weight (on logarithmic basis) for the solid cellulose residue and precipitate following several treatment conditions was studied using the corresponding SEC-based MMDs, which can be found in Appendix E. The curves showed a progressive decrease in the differential mass fraction of the residue at high DPs with increasing treatment time along with an increase in the fraction of low molecular mass polymers. In addition, the residue rapidly lost the bimodal shape observed in the initial MCC. These observations indicate a cleavage of the long polymer chains of cellulose, which has already been observed by Tolonen et al. (2013) using MMDs obtained by SEC, although the bimodal shape of MCC was maintained in their results.

These observations indicate that the hydrolysis of MCC under near-or supercritical conditions follow a random depolymerization mechanism. A random depolymerization would generate a molecular mass distribution which would follow

the Flory-Schulz formula (Equation 1, described in Section 2.1.4.). The fit of the data was tested against the molecular mass distribution of the water-soluble cello-oligosaccharides. The concentration of the water-soluble cello-oligosaccharides in the liquid product fractions obtained by anion-exchange chromatography at 360 °C is presented in Figure 18. The graph also shows the best fit of a Flory-Schulz distribution to the experimental data (dotted line).

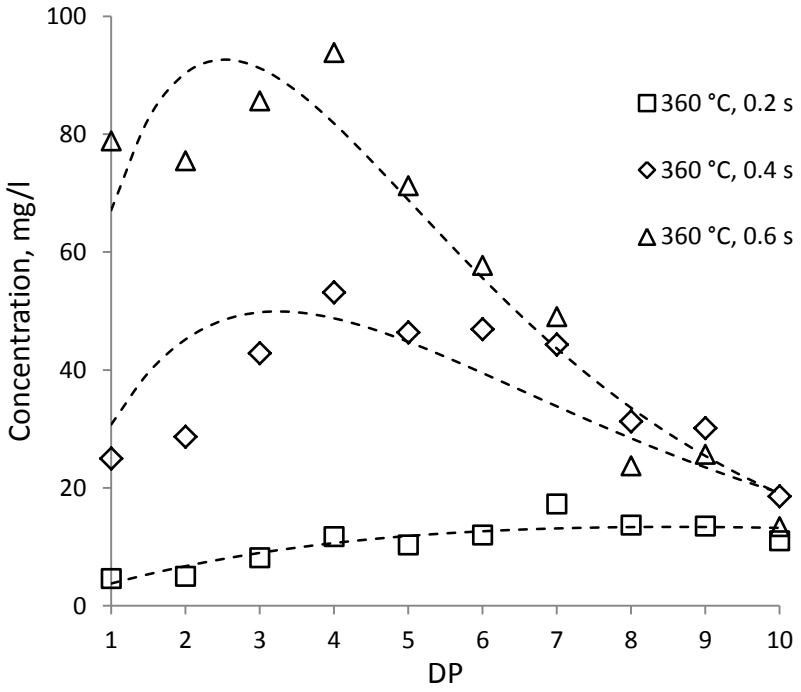

Figure 18. Formation of water-soluble cello-oligosaccharides.

The graph showed an overall increase in the concentration of COSs with increased reaction time. At low cellulose conversion the amount of COSs was low with relatively homogeneous distribution. At medium cellulose conversion the liquid fraction contained significantly more water-soluble COSs, with a distribution of concentrations centered on DP 4 to DP 6. At maximum cellulose conversion the amount of glucose and DP 2 to DP 4 oligomers increased and reached high concentration levels of about 80 mg/l each. However, the amount the solubilized higher oligomers (DP 7 to DP 10) only underwent a limited further increase.

These results show that further cellulose degradation increases the formation of glucose and all water-soluble cello-oligosaccharides, which are formed after

cleavage of longer cellulose chains. The good fit of the Flory-Schulz equation at each of the three displayed distributions indicates that the water-soluble cello-oligomers are produced by random depolymerization of microcrystalline cellulose. However, in order to prove a random polymerization the distribution of the whole cellulosic product must follow the Flory-Schulz distribution, including the solid precipitate fraction. The limited solubility for the higher DP oligosaccharides in ambient water causes some oligomers to be present in both fractions. The combined molecular mass distribution of the water-soluble cello-oligosaccharides and the solid precipitate is depicted in Figure 19. The distributions were adjusted according to the product yield of the fractions.

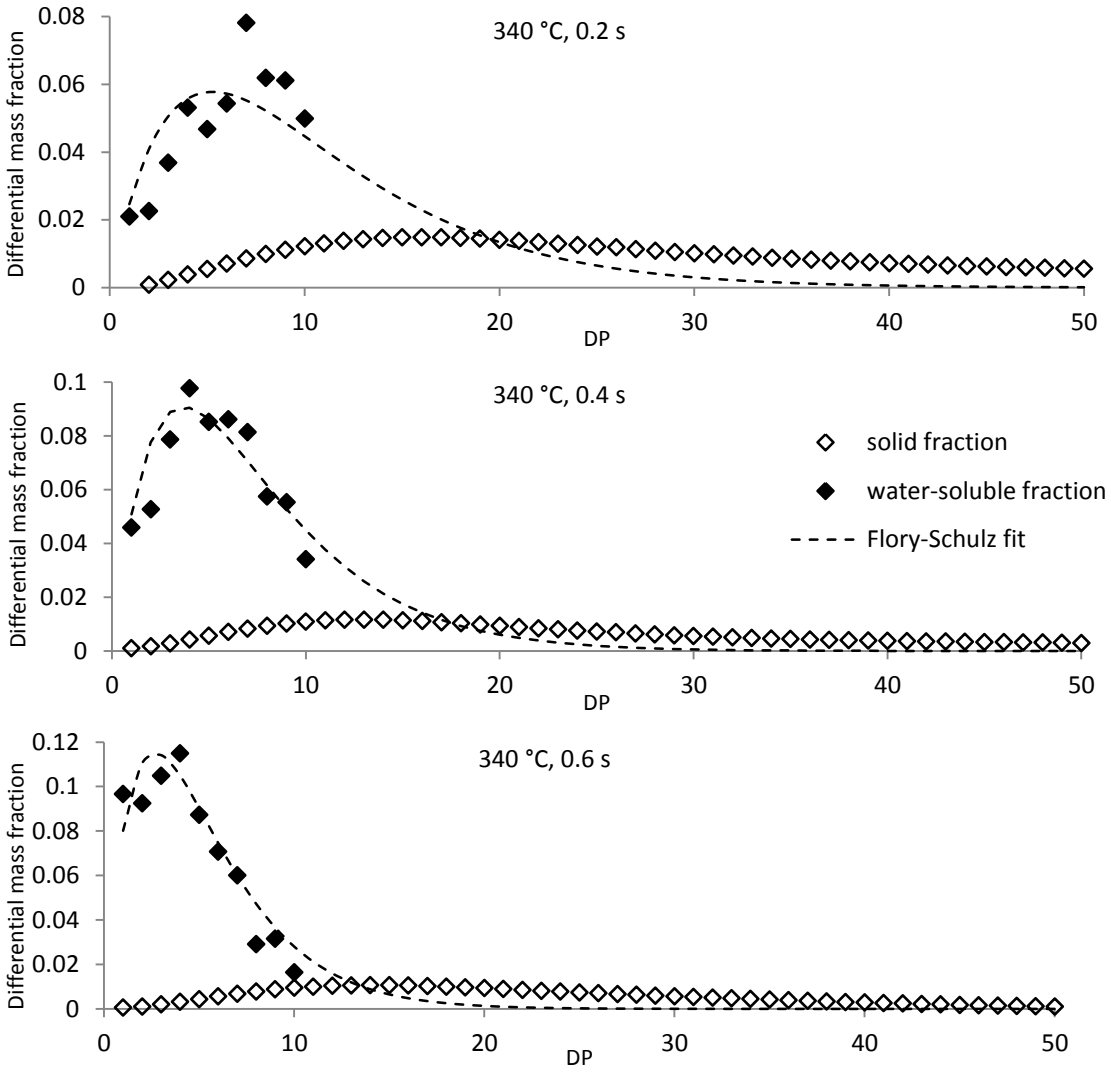

Figure 19. Evolution of low DPs with increasing treatment time.

The combined distributions showed a relatively good fit with the Flory-Schulz distribution for the water-soluble oligomers especially at high cellulose conversion. However, the model predicts a rapid decrease in the DMF at higher DPs, which was not observed experimentally. One reason for the discrepancy is that the molecular mass distribution of the precipitate was obtained using a size-exclusion chromatographic method and the detection technology designed and suitable for samples having a broad molecular mass distribution. In addition, with narrow distributions a phenomenon of band broadening has been reported due to chromatographic dispersion, which overestimates the differential mass fractions for the lowest and the highest molecular masses (Popovici et al. 2004). Therefore, repeating the analyses of the solid precipitate with a method which and more accurate at low molecular masses and more appropriate for narrow distributions would give more insights about the fit of the hydrolysis products with the assumed random depolymerization model.

4.4. PURIFICATION OF CELLO-OLIGOSACCHARIDES

The previous sections showed the potential of near-and supercritical treatment of microcrystalline cellulose for producing water-soluble cello-oligosaccharides. However, the product mass balance obtained by TOC analysis indicated that the liquid fraction also contained significant amounts of glucose and degradation products. Therefore, a subsequent purification step is required in order to utilize or recover the cello-oligomers. Various techniques have already been applied for this purpose (described in Section 2.2.3.), including solvent extraction, ion-exchange chromatography, and ultrafiltration. The latter presents several advantages, especially regarding the potential simplicity of the method. In addition this method allows concentrating the product mixtures by using membranes, which allow retaining the oligomers.

The purification of the COSs mixture produced by SCWT at 360 °C and for a residence time of 0.6s was performed in a simple filtration experiment (as described in Section 3.2.7.). The operation was repeated using three polyamide membranes

with MWCOs of 270 Da, 1000 Da, and 3000 Da, respectively. Figure 20 shows the retention of glucose and cello-oligomers with DPs up to 10 compared with the original sample.

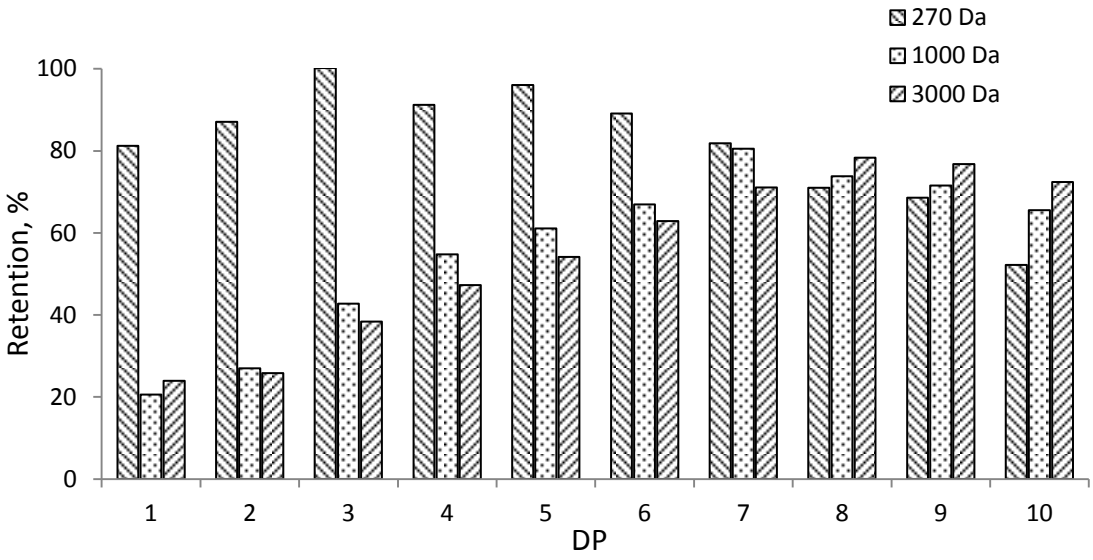

Figure 20. Retention of cello-oligosaccharides after ultrafiltration.

The highest retention was obtained for the membranes with a MWCO of 270 Da. Around 90 % of the DP 3 to DP 5 oligomers were retained. Glucose and cellobiose exhibited lower retention (80 % and 87 %, respectively), while the concentration of the higher DP oligomers gradually decreased. Similar patterns were observed for the two other membranes, which showed an increasing retention for higher molecular mass oligomers. Above a certain DP the ratio of the highest oligomers decreased. This was observed experimentally by the formation of a solid precipitate fraction in the retentate after the sample was filtrated, which confirms the lower solubility in ambient water for the oligomers with higher DPs.

In addition, TOC analysis of samples showed that for the 270 Da membrane the retentate fraction contained 82 % of the initial TOC of Simple filtration while retaining 95 % of the total DP 2 – DP 10 oligomer content of the sample. Therefore, ultrafiltration allowed the purification of the product sample from the low molar mass degradation products. In order to obtain further purified COSs solutions the effect of continuous filtration on the oligomer retetion was conducted (as described

in Section 3.2.7.). The 270 Da membrane was chosen as it exhibited the highest oligomer retention levels in simple filtration. The results of the continuous filtration are shown in Figure 21.

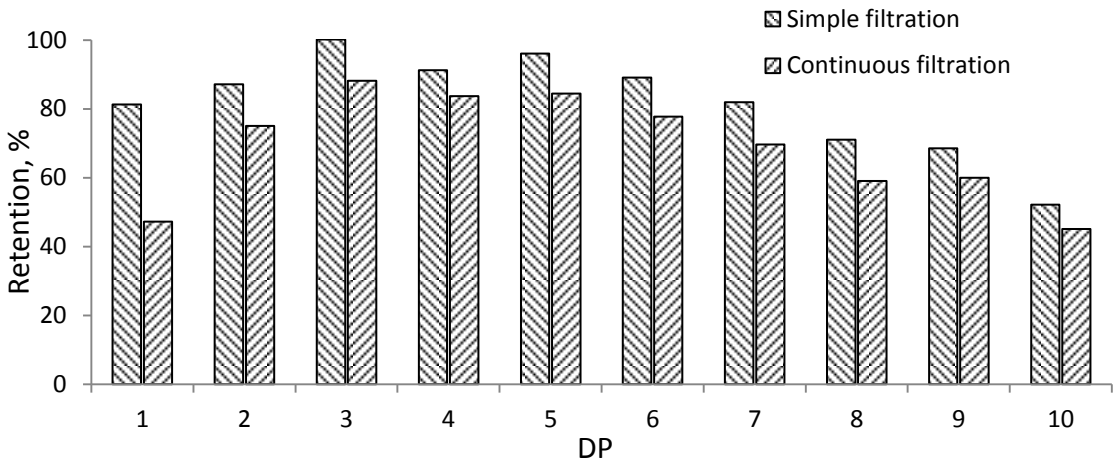

Figure 21. Effect of continuous ultrafiltration (270 Da) on the COSs retention.

Continuous filtration decreased the retention of all the cellulosic products in the sample as compared to single filtration. However, the retention was significantly lower for glucose (47 %) while the loss for oligomers was in the range of 5 % to 10 % only. The evolution of the concentration for glucose and the lower oligomers is similar to that already published in the literature for ultrafiltration of oligosaccharides mixtures using similar membranes. Goulas et al. (2003) reported a yield of 88 % for oligosaccharides after a four-stage filtration using membranes having a 50 % sodium chloride rejection. The results show that continuous filtration is an interesting method for removing the low molar mass contents of cello-oligosaccharides mixtures obtained after SCWT of microcrystalline cellulose. In the case of the 270 Da membrane it is believed that degradation products with molar masses below that of glucose can be efficiently removed using this technique. The selectivity of the method can be adjusted by filtration of the samples with membranes having various MWCO values, and the combined use of several membranes has been proposed in order to adjust the mixture to the desired concentrations (Nabarlatz et al. 2007).

4.5. PROCESS COST STRUCTURE

High-purity, analytical grade cello-oligosaccharides are today commercially available from cellobiose to cellohexaose (DP 2 to DP 6). However, the difficulty to produce, purify and fractionate the COSs impedes their availability and restrains the development of novel uses for cello-oligomers. As a consequence, their observed price can reach several thousands of Euros per gram for individual compounds of high purity; such compounds find uses as standards in analytical chemistry and biochemistry (Zhang & Lynd 2003). Other oligosaccharides are more easily produced from other biomass sources than lignocellulosic biomass; however, the use of agriculture feedstock, such as corn or sugarcane is criticized as these raw materials can also produce food. In this context the main benefits of supercritical water treatment of cellulose, which include continuous production, fast reaction time and water as the sole reagent and solvent, combined with simple, water-based purification and fractionation techniques, are believed to make it a serious alternative for producing cello-oligosaccharides at commercial scale.

The results presented in the previous sections show that a process consisting of a SCWT followed by purification using ultrafiltration and fractionation using ion-exchange chromatography is a fast and efficient method for producing cello-oligosaccharides and low molecular mass cellulose. However, the pilot-scale reactor system used in this study requires significant capital and operating costs, which need to be estimated.

The estimations for capital and operating costs of the process presented in Section 3.2.8. are shown in Figure 22. The operating costs are expressed per kilogram of microcrystalline cellulose, equivalent to a continuous production of 15 days.

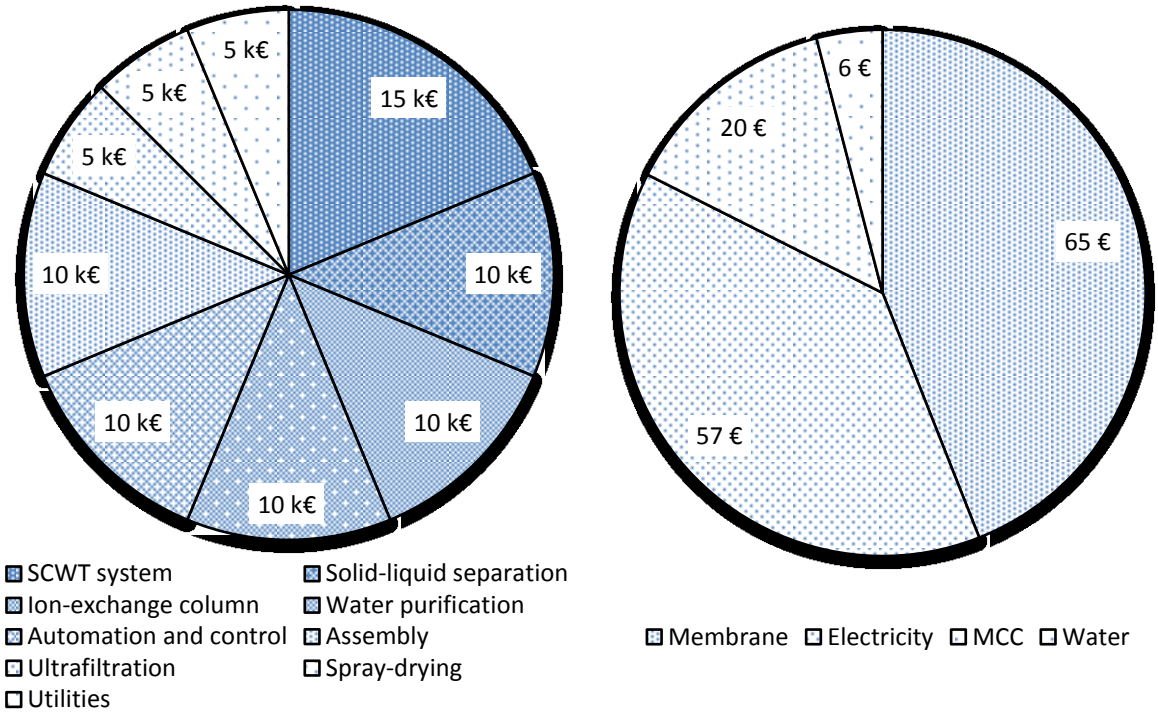

Figure 22. Capital and operating costs.

According to the hypotheses and design parameters the cost structure analysis shows that an integrated SCWT process initially able to process 1 kg of MCC in 15 days would require around 80 k€ in initial investment and would cost nearly 150 € in operating costs. The processing of 1 kg of MCC produces about 50 grams of each cello-oligosaccharide from DP 2 to DP 6, in addition to 80 g of higher water-soluble oligomers, 55 grams of glucose, and 10 g of water-insoluble low DP cellulose precipitate.

Although the capital costs are not easily compressible, the membranes and the raw material have some potential for economies of scale. In addition, various process improvements can be identified, which reduce the operating costs and increase the product output. These optimizations include increasing the initial MCC consistency, decreasing the quenching flow, reusing the residual cellulose, and recovering part of the energy lost in product cooling to preheat the cellulose and heating flows. Using already available energy sources, such as low-pressure steam from a pulp mill, would also reduce the process costs, as electricity accounts for nearly 40 % of the total operating costs needed to produce the cello-oligosaccharides.

5. CONCLUSIONS

This thesis investigated the degradation of microcrystalline cellulose in near- and supercritical water at 250 bar and under a wide range of temperatures and treatment times. The objective was to characterize the product as well as to investigate whether the product distribution can be optimized for cello-oligosaccharides production by adjusting the treatment time and temperature. Four fractions were isolated from the product samples, which were analyzed according to various gravimetric and chromatographic techniques. The results of the analyses provided information about the composition of the samples in terms of water-soluble and water-insoluble materials as well as the molecular mass distribution of the products.

The results were in accordance with previously published literature. It was found that the cellulose degradation in near- and supercritical water seems to follow a first-order Arrhenius-type of reaction with an activation energy around 120 kJ/mol. In addition, cellulose polymers accounted for most of the product compounds and were found under three forms: undissolved, degraded cellulose residue, low molecular mass cellulose polymers soluble in supercritical water but insoluble in ambient water (with a DP_w around 25), and cello-oligosaccharides soluble in ambient water. In addition, the TOC-based mass balance of the samples indicated that a significant fraction of the initial MCC was further degraded into unidentified, cellulose-derived products.

The evolution of the concentration of precipitate as well as the concentration and DP_w of cellulose residue with increased cellulose conversion suggest that the degradation mechanism can be divided into two steps: the heterogeneous depolymerization of cellulose into polymers that are solubilized in supercritical water, and the further homogeneous conversion of these solubilized polymers into cello-oligomers and other degradation products. The treatment temperature was found to have little influence on the reaction pathway and the evolution of the DP of the products resulted solely of the degree of conversion of the initial cellulose.

Based on these results it is suggested that the depolymerization is largely taking place during homogeneous hydrolysis, which is triggered by the treatment conditions. Furthermore, evidence was found that the cellulose depolymerization mechanism involves random hydrolysis of the glycosidic bonds of the cellulose chains, based on the fit of the experimental cello-oligosaccharides concentrations to the Flory-Schulz equation.

The amount of produced water-soluble cello-oligosaccharides reached up to 575 mg/l at 360 °c and 0.6 s. The solid precipitate fraction was formed up to 250 mg/l at 360 °C and 0.4 s. The corresponding yields with an initial cellulose consistency of 0.5 %wt were about 5.7 % and 2.5 %, respectively. These products were obtained with treatment times shorter than one second and using water as the sole reagent. Therefore, these results show that the near- and supercritical water treatment of cellulose is a fast, environmentally-friendly and potentially scalable treatment for producing cello-oligosaccharides.

However, the low used consistencies as well as the important amount of degradation products call for the development of a purification and separation method. Ultrafiltration experiments performed with a batch stirred-cell using polyamide membranes with molecular-weight cut-offs comprised between 270 and 3000 Da proved to be a potentially efficient method, as the amount low molar mass components were significantly decreased while retaining more than 80 % of the oligomers.

Various studies have proved the health-related benefits of cello-oligosaccharides when added to food as prebiotics. However, their cost-efficient mass production today remains a challenge and the availability of pure cello-oligosaccharides is restricted to analytic uses, with current retail prices in the order of several thousand Euros per gram. This thesis proved that the hydrothermal treatment of cellulose under near- or supercritical conditions is a potential method for producing cello-oligosaccharides at large scale, thus enabling their use as prebiotics in food as well as the development of new applications.

This thesis highlighted the need for further research related to the near-and supercritical treatment of cellulose. The extent to which the dissolution of cellulose is affecting the hydrolysis and the formation of cellulosic fractions, as well as the overall kinetic mechanism in near-critical and supercritical conditions remain unclear. In addition, little is known about the degradation behavior of cellulose at extended treatment conditions, such as under significantly higher pressure and temperature ranges. Furthermore, the development of a cello-oligosaccharides production sequence involving hydrothermal treatment requires further investigation, including process optimizations, the use of the low DP cellulose II precipitate fraction as a side product of the treatment, as well as and the development of an efficient method for fractionating the oligosaccharides into pure individual components.

6. REFERENCES

Akpınar, Ö. & Penner, M.H. 2004, "Preparation and Separation of Food Grade Cellooligosaccharides", *GOÜ. Ziraat Fakültesi Dergisi,* vol. 27, no. 1, pp. 27-32.

Akpinar, O. 2002, *Preparation and modification of cellooligosaccharides*, Oregon State University.

Aksoy, B. 2011, *Hydrothermale Herstellung von Regeneratcellulose*, M.Sc. thesis, Karlsruher Institut für Technologie.

Benoit, M., Rodrigues, A., De, O.V., Fourre, E., Barrault, J., Tatibouet, J. & Jerome, F. 2012, "Combination of ball-milling and non-thermal atmospheric plasma as physical treatments for the saccharification of microcrystalline cellulose", *Green Chemistry,* vol. 14, no. 8, pp. 2212-2215.

Bergenstråhle, M., Wohlert, J., Himmel, M.E. & Brady, J.W. 2010, "Simulation studies of the insolubility of cellulose", *Carbohydrate research,* vol. 345, no. 14, pp. 2060-2066.

Berggren, R. 2003, *Cellulose degradation in pulp fibers studied as changes in molar mass distributions*, Fiber- och polymerteknologi.

Cantero, D.A., Bermejo, M.D. & Cocero, M.J. 2013, "Kinetic analysis of cellulose depolymerization reactions in near critical water", *The Journal of Supercritical Fluids,* vol. 75, no. 0, pp. 48-57.

Ciolacu, D. & Popa, V.I. 2010, *Polymer Science and Technology : Cellulose Allomorphs : Structure, Accessibility and Reactivity,* Nova Science Publishers, Inc., Hauppauge, NY, USA.

Deguchi, S., Tsujii, K. & Horikoshi, K. 2006, "Cooking cellulose in hot and compressed water", *Chemical communications (Cambridge, England),* vol. (31), no. 31, pp. 3293-3295.

Deguchi, S., Tsujii, K. & Horikoshi, K. 2008, "Crystalline-to-amorphous transformation of cellulose in hot and compressed water and its implications for hydrothermal conversion", *Green Chemistry,* vol. 10, no. 2, pp. 191-196.

Deguchi, S., Tsujii, K. & Horikoshi, K. 2008, "Effect of acid catalyst on structural transformation and hydrolysis of cellulose in hydrothermal conditions", *Green Chemistry,* vol. 10, no. 6, pp. 623-626.

Ehara, K. & Saka, S. 2002, "A comparative study on chemical conversion of cellulose between the batch-type and flow-type systems in supercritical water", *Cellulose,* vol. 9, no. 3-4, pp. 301-311.

Fernandes, A.N., Thomas, L.H., Altaner, C.M., Callow, P., Forsyth, V.T., Apperley, D.C., Kennedy, C.J. & Jarvis, M.C. 2011, "Nanostructure of cellulose microfibrils in spruce wood", *Proceedings of the National Academy of Sciences,* vol. 108, no. 47, pp. E1195-E1203.

Flory, P.J. 1936, "Molecular Size Distribution in Linear Condensation Polymers", *Journal of the American Chemical Society,* vol. 58, no. 10, pp. 1877-1885.

Galkin, A. & Lunin, V. 2005, "Subcritical and supercritical water: a universal medium for chemical reactions", *Russian Chemical Reviews,* vol. 74, no. 1, pp. 21.

Gardner, K.H. & Blackwell, J. 1974, "The structure of native cellulose", *Biopolymers,* vol. 13, no. 10, pp. 1975-2001.

Goulas, A.K., Grandison, A.S. & Rastall, R.A. 2003, "Fractionation of oligosaccharides by nanofiltration", *Journal of the science of food and agriculture,* vol. 83, no. 7, pp. 675-680.

Goulas, A.K., Kapasakalidis, P.G., Sinclair, H.R., Rastall, R.A. & Grandison, A.S. 2002, "Purification of oligosaccharides by nanofiltration", *Journal of Membrane Science,* vol. 209, no. 1, pp. 321-335.

Gray, M., Converse, A. & Wyman, C. 2003, "Sugar monomer and oligomer solubility", *Applied Biochemistry and Biotechnology,* vol. 105, no. 1-3, pp. 179-193.

Gross, A.S. & Chu, J. 2010, "On the Molecular Origins of Biomass Recalcitrance: The Interaction Network and Solvation Structures of Cellulose Microfibrils", *The Journal of Physical Chemistry B,* vol. 114, no. 42, pp. 13333-13341.

Guo, Y., Wang, S.Z., Xu, D.H., Gong, Y.M., Ma, H.H. & Tang, X.Y. 2010, "Review of catalytic supercritical water gasification for hydrogen production from biomass", *Renewable and Sustainable Energy Reviews,* vol. 14, no. 1, pp. 334-343.

Hauru, L.K.J., Hummel, M., King, A.W.T., Kilpeläinen, I. & Sixta, H. 2012, "Role of Solvent Parameters in the Regeneration of Cellulose from Ionic Liquid Solutions", *Biomacromolecules,* vol. 13, no. 9, pp. 2896-2905.

Hearle, J.W.S. 1958, "A fringed fibril theory of structure in crystalline polymers", Journal of Polymer Science, vol. 28, no. 117, pp. 432-435.

Huang, Y. & Fu, Y. 2013, "Hydrolysis of cellulose to glucose by solid acid catalysts", Green Chemistry, vol. 15, no. 5, pp. 1095-1111.

Huebner, A., Ladisch, M.R. & Tsao, G.T. 1978, "Preparation of cellodextrins: An engineering approach", *Biotechnology and bioengineering,* vol. 20, no. 10, pp. 1669-1677.

Jasiukaityte-Grojzdek, E., Kunaver, M. & Poljansek, I. 2012, "Influence of cellulose polymerization degree and crystallinity on kinetics of cellulose degradation", *BioResources,* vol. 7, no. 3.

Kamler, J. & Soria, J.A. 2012, *Supercritical Water Gasification of Municipal Sludge: A Novel Approach to Waste Treatment and Energy Recovery, Gasification for Practical Applications,* Dr. Yong Seung Yun edn.

Klemm, D., Heublein, B., Fink, H. & Bohn, A. 2005, "Cellulose: Fascinating Biopolymer and Sustainable Raw Material", *Angewandte Chemie International Edition,* vol. 44, no. 22, pp. 3358-3393.

Kumar, S. & Gupta, R.B. 2008, "Hydrolysis of Microcrystalline Cellulose in Subcritical and Supercritical Water in a Continuous Flow Reactor", *Industrial & Engineering Chemistry Research,* vol. 47, no. 23, pp. 9321-9329.

Kupiainen, L., Ahola, J. & Tanskanen, J. 2012, "Distinct Effect of Formic and Sulfuric Acids on Cellulose Hydrolysis at High Temperature", *Industrial & Engineering Chemistry Research,* vol. 51, no. 8, pp. 3295-3300.

Lavoine, N., Desloges, I., Dufresne, A. & Bras, J. 2012, "Microfibrillated cellulose – Its barrier properties and applications in cellulosic materials: A review", *Carbohydrate Polymers,* vol. 90, no. 2, pp. 735-764.

Lemmon, E.W., McLinden, M.O. & Friend, D.G. "Thermophysical Properties of Fluid Systems" in *NIST Chemistry WebBook, NIST Standard Reference Database Number 69*, P.J. Linstrom and W.G. Mallard, National Institute of Standards and Technology, Gaithersburg MD, 20899.

Lin, C., Conner, A.H. & Hill, C.G. 1993, "The heterogeneous, dilute-acid hydrolysis of cellulose", eds. J.F. Kennedy, G.O. Phillips & P.A. Williams, Ellis Horwood, New York, pp. 177-182.

Marshall, W.L. & Franck, E.U. 1981, "Ion product of water substance, 0–1000 °C, 1–10,000 bars New International Formulation and its background", *Journal of Physical and Chemical Reference Data,* vol. 10, no. 2, pp. 295-304.

Medronho, B. & Lindman, B. "Brief overview on cellulose dissolution/regeneration interactions and mechanisms", *Advances in Colloid and Interface Science*.

Millet, M.A., Moore, W.E. & Saeman, J.E. 1954, "Preparation and Properties of Hydrocelluloses", *Industrial & Engineering Chemistry,* vol. 46, no. 7, pp. 1493-1497.

Mountzouris, K.C., Gilmour, S.G., Grandison, A.S. & Rastall, R.A. 1999, "Modeling of oligodextran production in an ultrafiltration stirred-cell membrane reactor", *Enzyme and microbial technology,* vol. 24, no. 1–2, pp. 75-85.

Nabarlatz, D., Torras, C., Garcia-Valls, R. & Montané, D. 2007, "Purification of xylo-oligosaccharides from almond shells by ultrafiltration", *Separation and Purification Technology,* vol. 53, no. 3, pp. 235-243.

Nada, A.M.A., El-Kady, M., El-Sayed, E. & Amine, F.M. 2009, "Preparation and characterization of microcrystalline cellulose (MCC)", *BioResources; Vol 4, No 4*.

Navard, P. & Cuissinat, C. 2006, "Cellulose swelling and dissolution as a tool to study the fiber structure ", *7th International Symposium "Alternative Cellulose : Manufacturing, Forming, Properties*Rudolstadt, Germany.

Nishiyama, Y., Sugiyama, J., Chanzy, H. & Langan, P. 2003, "Crystal Structure and Hydrogen Bonding System in Cellulose Iβ from Synchrotron X-ray and Neutron Fiber Diffraction", *Journal of the American Chemical Society,* vol. 125, no. 47, pp. 14300-14306.

Olsson, C. & Westman, G. 2013, "Direct Dissolution of Cellulose: Background, Means and Applications" in *Cellulose - Fundamental Aspects*, Theo G.M. Van De Ven edn.

Park, S., Baker, J.O., Himmel, M.E., Parilla, P.A. & Johnson, D.K. 2010, "Cellulose crystallinity index: measurement techniques and their impact on interpreting cellulase performance", *Biotechnology for Biofuels,* vol. 3, no. 10.

Payne, C.M., Himmel, M.E., Crowley, M.F. & Beckham, G.T. 2011, "Decrystallization of Oligosaccharides from the Cellulose II Surface with Molecular Simulation", *The Journal of Physical Chemistry Letters,* vol. 2, no. 13, pp. 1546-1550.

Peri, S., Muthukumar, L., Nazmul Karim, M. & Khare, R. 2012, "Dynamics of cello-oligosaccharides on a cellulose crystal surface", *Cellulose,* vol. 19, no. 6, pp. 1791-1806.

Peterson, A.A., Vogel, F., Lachance, R.P., Froling, M., Antal, J.,Michael J. & Tester, J.W. 2008, "Thermochemical biofuel production in hydrothermal media: A review of sub- and supercritical water technologies", *Energy & Environmental Science,* vol. 1, no. 1, pp. 32-65.

Popovici, S., Kok, W.T. & Schoenmakers, P.J. 2004, "Band broadening in size-exclusion chromatography of polydisperse samples", *Journal of Chromatography A,* vol. 1060, no. 1–2, pp. 237-252.

Russell, J.B. 1985, "Fermentation of cellodextrins by cellulolytic and noncellulolytic rumen bacteria", *Applied and environmental microbiology,* vol. 49, no. 3, pp. 572-576.

Sasaki, M., Adschiri, T. & Arai, K. 2004, "Kinetics of cellulose conversion at 25 MPa in sub- and supercritical water", *AIChE Journal,* vol. 50, no. 1, pp. 192-202.

Sasaki, M., Adschiri, T. & Arai, K. 2003, "Production of Cellulose II from Native Cellulose by Near- and Supercritical Water Solubilization", *Journal of Agricultural and Food Chemistry,* vol. 51, no. 18, pp. 5376-5381.

Sasaki, M., Fang, Z., Fukushima, Y., Adschiri, T. & Arai, K. 2000, "Dissolution and Hydrolysis of Cellulose in Subcritical and Supercritical Water", *Industrial & Engineering Chemistry Research,* vol. 39, no. 8, pp. 2883-2890.

Sasaki, M., Kabyemela, B., Malaluan, R., Hirose, S., Takeda, N., Adschiri, T. & Arai, K. 1998, "Cellulose hydrolysis in subcritical and supercritical water", *The Journal of Supercritical Fluids,* vol. 13, no. 1–3, pp. 261-268.

Sharples, A. 1957, "The hydrolysis of cellulose and its relation to structure", Transactions of the Faraday Society, vol. 53, no. 0, pp. 1003-1013.

Shaw, R.W., Brill, T.B., Clifford, A.A., Eckert, C.A. & Franck, E.U. 1991, "Supercritical water: A medium for chemistry", *Chemical and Engineering News,* vol. 69, no. 51, pp. 26-39.

Sınağ, A., Gülbay, S., Uskan, B. & Güllü, M. 2009, "Comparative studies of intermediates produced from hydrothermal treatments of sawdust and cellulose", *The Journal of Supercritical Fluids,* vol. 50, no. 2, pp. 121-127.

Sixta, H. 2006, *Handbook of Pulp,* Wiley-VCH Verlag.

Stupińska, H., Iller, E., Zimek, Z., Wawro, D., Ciechańska, D., Kopania, E., Palenik, J., Milczarek, S., Stęplewski, W. & Krzyżanowska, G. 2007, "An Environment-Friendly Method to Prepare Microcrystalline Cellulose", *FIBRES & TEXTILES in Eastern Europe,* vol. 15, no. 5-6 (64-65), pp. 167-172.

Taherzadeh, M.J. & Karimi, K. 2007, "Acid-based hydrolysis processes for ethanol from lignocellulosic materials: A review", *BioResources, 2007, Vol.2(3), pp.472-499,* vol. 2, no. 3, pp. 472-499.

Tolonen, L.K., Zuckerstätter, G., Penttilä, P.A., Milacher, W., Habicht, W., Serimaa, R., Kruse, A. & Sixta, H. 2011, "Structural Changes in Microcrystalline Cellulose in Subcritical Water Treatment", *Biomacromolecules,* vol. 12, no. 7, pp. 2544-2551.

Tolonen, L., Penttilä, P., Serimaa, R., Kruse, A. & Sixta, H. 2013, "The swelling and dissolution of cellulose crystallites in subcritical and supercritical water", *Cellulose,* vol. 20, no. 6, pp. 2731-2744.

Uematsu, M. & Frank, E.U. 1980, "Static Dielectric Constant of Water and Steam", *Journal of Physical and Chemical Reference Data,* vol. 9, no. 4, pp. 1291-1306.

Vega, J., Meira, G. & Yossen, M. 2004, "Gel Permeation and Size Exclusion Chromatography" in CRC Press, pp. 827-869.

Wahlstrom, R., Rovio, S. & Suurnakki, A. 2012, "Partial enzymatic hydrolysis of microcrystalline cellulose in ionic liquids by Trichoderma reesei endoglucanases", *RSC Advances,* vol. 2, no. 10, pp. 4472-4480.

Wang, C., Zhou, F., Yang, Z., Wang, W., Yu, F., Wu, Y. & Chi, R. 2012, "Hydrolysis of cellulose into reducing sugar via hot-compressed ethanol/water mixture", *Biomass and Bioenergy,* vol. 42, pp. 143-150.

Wyman, C., Decker, S., Himmel, M., Brady, J., Skopec, C. & Viikari, L. 2004, "Hydrolysis of Cellulose and Hemicellusose", CRC Press.

Yang, B., Dai, Z., Ding, S. & Wyman, C.E. 2011, "Enzymatic hydrolysis of cellulosic biomass", *Biofuels,* vol. 2, no. 4, pp. 421-450.

Yang, B. & Wyman, C.E. 2008, "Pretreatment: the key to unlocking low-cost cellulosic ethanol", *Biofuels, Bioproducts and Biorefining,* vol. 2, no. 1, pp. 26-40.

Yu, Y. & Wu, H. 2010, "Understanding the Primary Liquid Products of Cellulose Hydrolysis in Hot-Compressed Water at Various Reaction Temperatures", *Energy Fuels,* vol. 24, no. 3, pp. 1963-1971.

Yu, Y. & Wu, H. 2009, "Characteristics and Precipitation of Glucose Oligomers in the Fresh Liquid Products Obtained from the Hydrolysis of Cellulose in Hot-Compressed Water", *Industrial & Engineering Chemistry Research,* vol. 48, no. 23, pp. 10682-10690.

Zhang, Y.P. & Lynd, L.R. 2003, "Cellodextrin preparation by mixed-acid hydrolysis and chromatographic separation", *Analytical Biochemistry,* vol. 322, no. 2, pp. 225-232.

Zhu, S., Wu, Y., Chen, Q., Yu, Z., Wang, C., Jin, S., Ding, Y. & Wu, G. 2006, "Dissolution of cellulose with ionic liquids and its application: a mini-review", *Green Chemistry,* vol. 8, no. 4, pp. 325-327.

Zugenmaier, P. 2008, *Crystalline cellulose and derivatives characterization and structures,* Springer, Berlin.

7. APPENDIX

Appendix A: Generalities

a) Nomenclature for cello-oligosaccharides

DP	Usual name
1	Glucose
2	Cellobiose
3	Cellotriose
4	Cellotetraose
5	Cellopentaose
6	Cellohexaose
7	Celloheptaose
8	Cellooctaose
9	Cellononaose
10	Cellodecaose
11	Celloundecaose
12	Cellododecaose

b) Physical properties of water at 250 bar

Temperature, °C	Density, kg/m^3	Specific enthalpy, kJ/kg	Ion product, $-\log_{10}$	Dielectric constant	Viscosity, mPa.s
20	1009	107	14.2	88.3	0.993
320	703	1439	11.4	27.4	0.084
340	655	1558	11.6	25.6	0.077
360	589	1699	12.1	24.7	0.068
380	451	1936	13.6	22.4	0.052
390	215	2396	16.5	21.7	0.032
500	90	3166	22.4	15.2	0.031

Appendix B: SCWT reactor system

a) Operating procedure for the SCWT system

The procedure for producing samples consisted of four phases: heating-up, sampling, cooling-down, and cleaning. The system operation started with deionized water only. During the heating-up phase, the reactor and the preheater were first set at a temperature of 90 °C for at least one hour, in order to remove any residual water from the system. The pumps were then turned on, the back-pressure regulator adjusted to the desired pressure, and the pressure dampers opened. After control of the flows and temperature stabilization, the temperature of the preheater was slowly increased up to the desired temperature by steps of 50 °C increase every 20 minutes, in order to minimize the mechanical stress due to temperature changes in the system. The temperature of the reactor heating elements was increased accordingly in order to match the displayed temperature at the core of the reactor.

Once the system reached the desired reaction temperature range, the sampling phase first consisted in adding cellulose suspension into the cellulose tank. The suspension was prepared and stirred for at least one hour before the addition, and dilution in the tank taken into account in its consistency. The system was then let to stabilize and finely adjusted at the desired temperature. Once in a steady state the sampling was performed according to the experimental procedure detailed in Section 3.2.2. If samples were taken at several reaction temperatures or residence times with the same suspension the preheating and reactor temperatures were first adjusted as well as the pump stroke lengths, and the system was let to reach a steady state before sampling.

The cooling-down phase took place after all the desired samples were collected. The heating water flow was set to maximum, and the preheater was turned off until the reaction temperature reached values below 100 °C. Finally, the cleaning phase included several steps of emptying the cellulose tank to a low liquid level and diluting the suspension with deionized water until the liquid in the cellulose tank was clear. The pumps were then turned off, and the back-pressure regulator was opened and cleaned from any cellulose deposit than may have been formed during the operation.

b) Pump surface fits for the function mass flow = f(frequency, stroke length)

Cellulose pump:

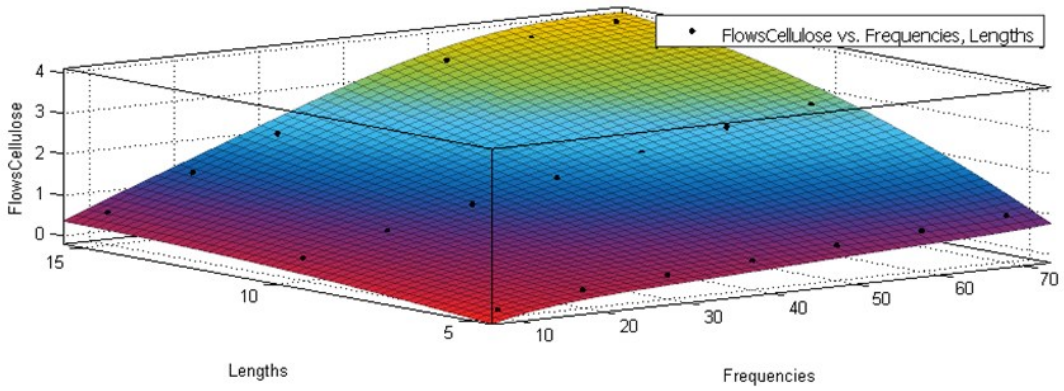

Preheating pump:

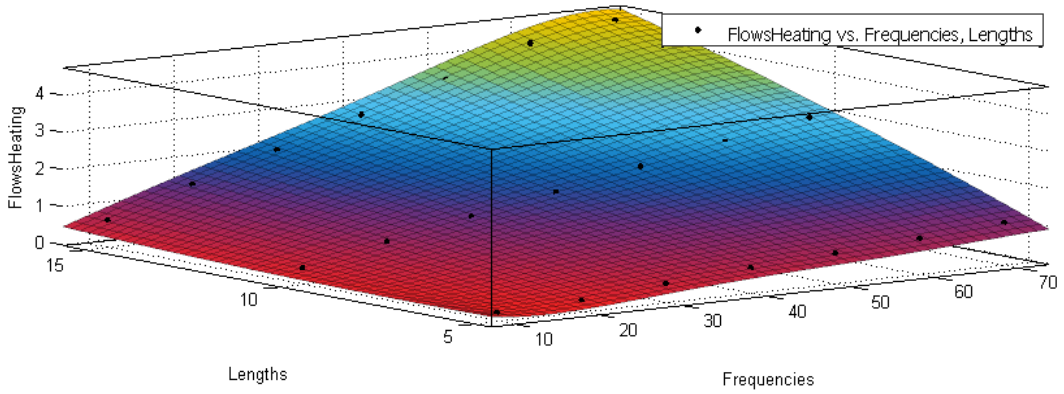

Quenching pump:

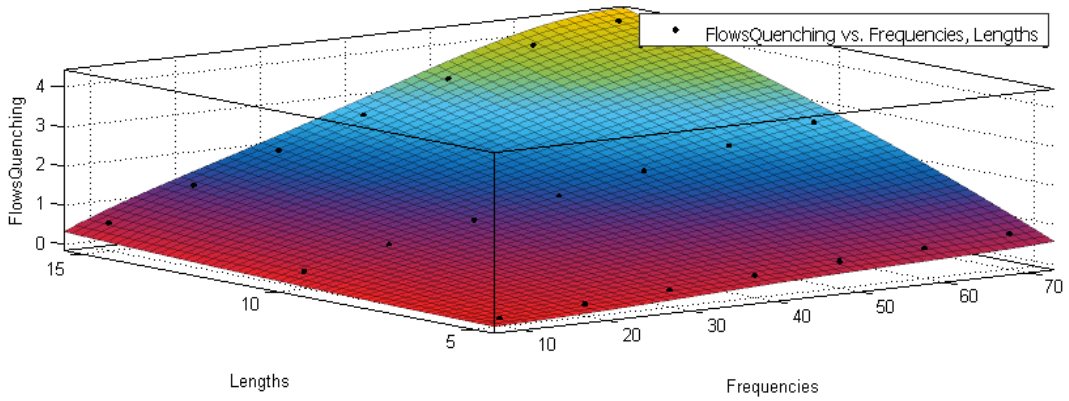

c) Measured vs. projected total pump mass flows

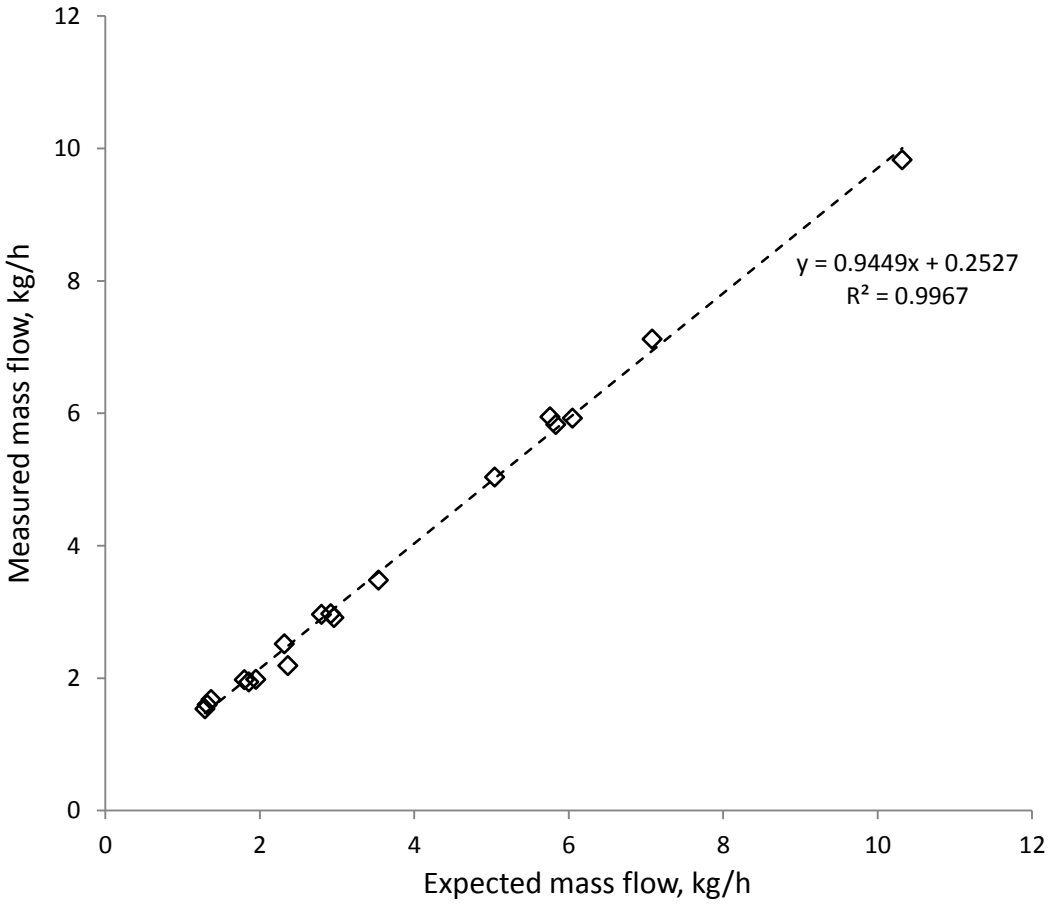

Appendix C: Sampling analysis scheme

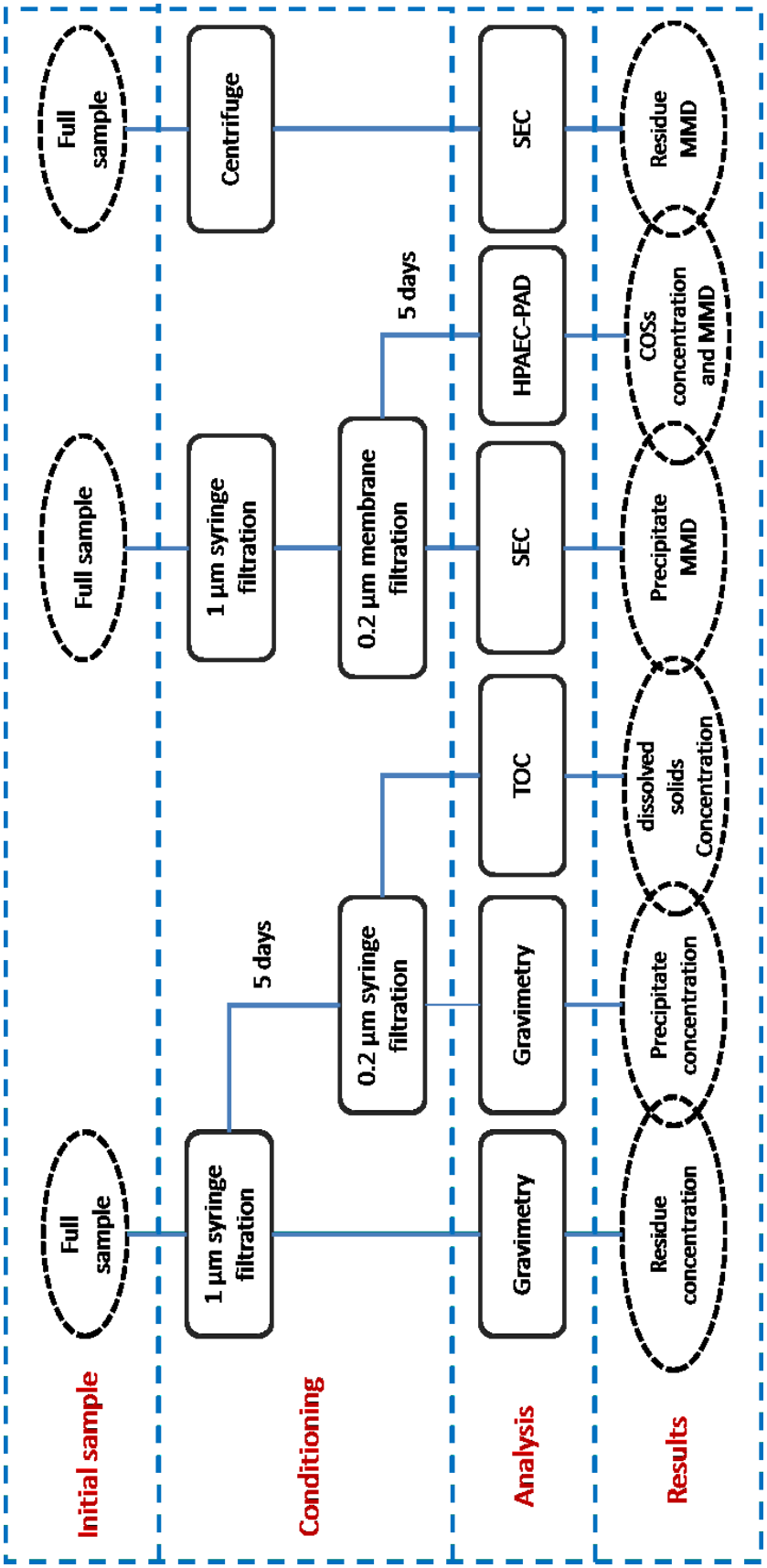

Appendix D: HPAEC-PAD calibration

a) Calibration curves for glucose and DP 1 – DP 6 oligomers

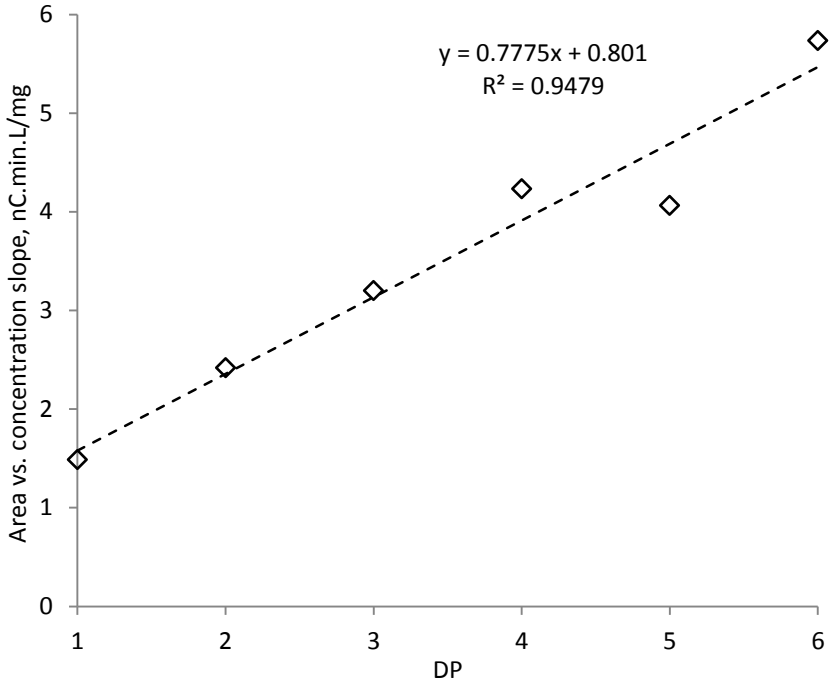

a) Extrapolation curve for the calibration of DP 7 - DP 10 oligomers

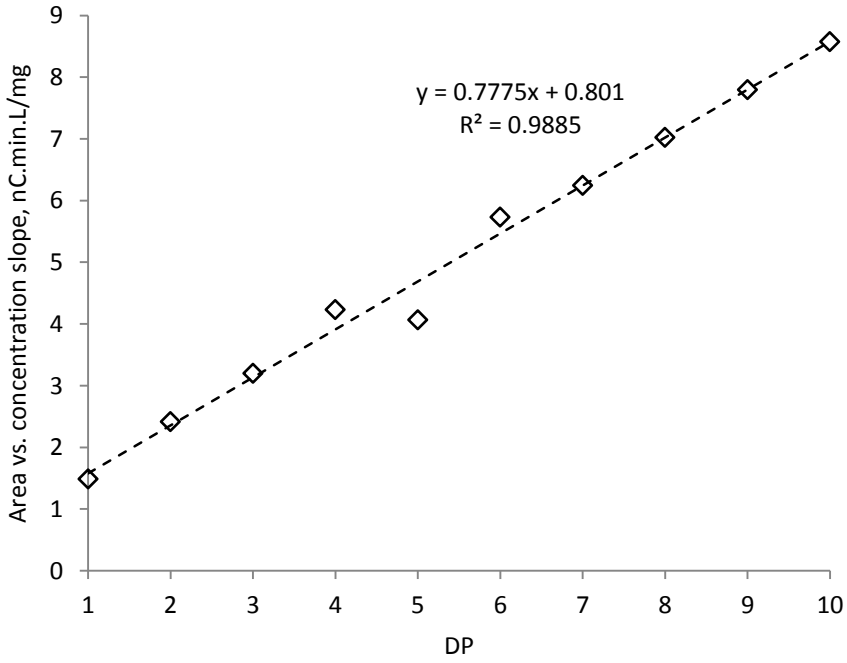

Appendix E: Results

a) Experimental plan and numerical values for the product fractions

Sample	Temperature	Time	Cellulose conversion	Solid residue	Solid precipitate	Water-soluble oligomers	Water-soluble degradation products	Residue DPw	Precipitate DPw
#	°C	s	%	mg/l	mg/l	mg/l	mg/l	-	-
1	320	0.2	12.1	1309	49	48	83	84	309
2	320	0.4	27.1	1056	129	146	118	33	242
3	320	0.6	40.8	695	126	224	129	26	189
4	320	0.8	52.1	417	105	241	108	24	166
5	340	0.2	18.3	1136	114	53	88	66	281
6	340	0.4	43.7	627	177	183	128	29	185
7	340	0.6	88.4	120	243	499	174	21	112
8	340	0.8	98.9	10	46	530	296	21	-
9	360	0.2	30.7	783	145	107	94	24	223
10	360	0.4	82.7	157	246	367	141	24	91
11	360	0.6	99.2	7	15	575	401	18	-
12	380	0.1	53.6	468	221	148	172	70	176
13	380	0.2	65.0	344	190	247	201	28	85
14	380	0.4	91.5	70	146	346	261	23	-
15	380	0.6	98.4	12	15	356	411	-	-
16	390	0.1	55.0	398	218	109	160	61	196
17	390	0.2	80.5	181	234	249	266	30	143
18	390	0.3	92.3	65	194	334	251	25	101

b) Product mass balance

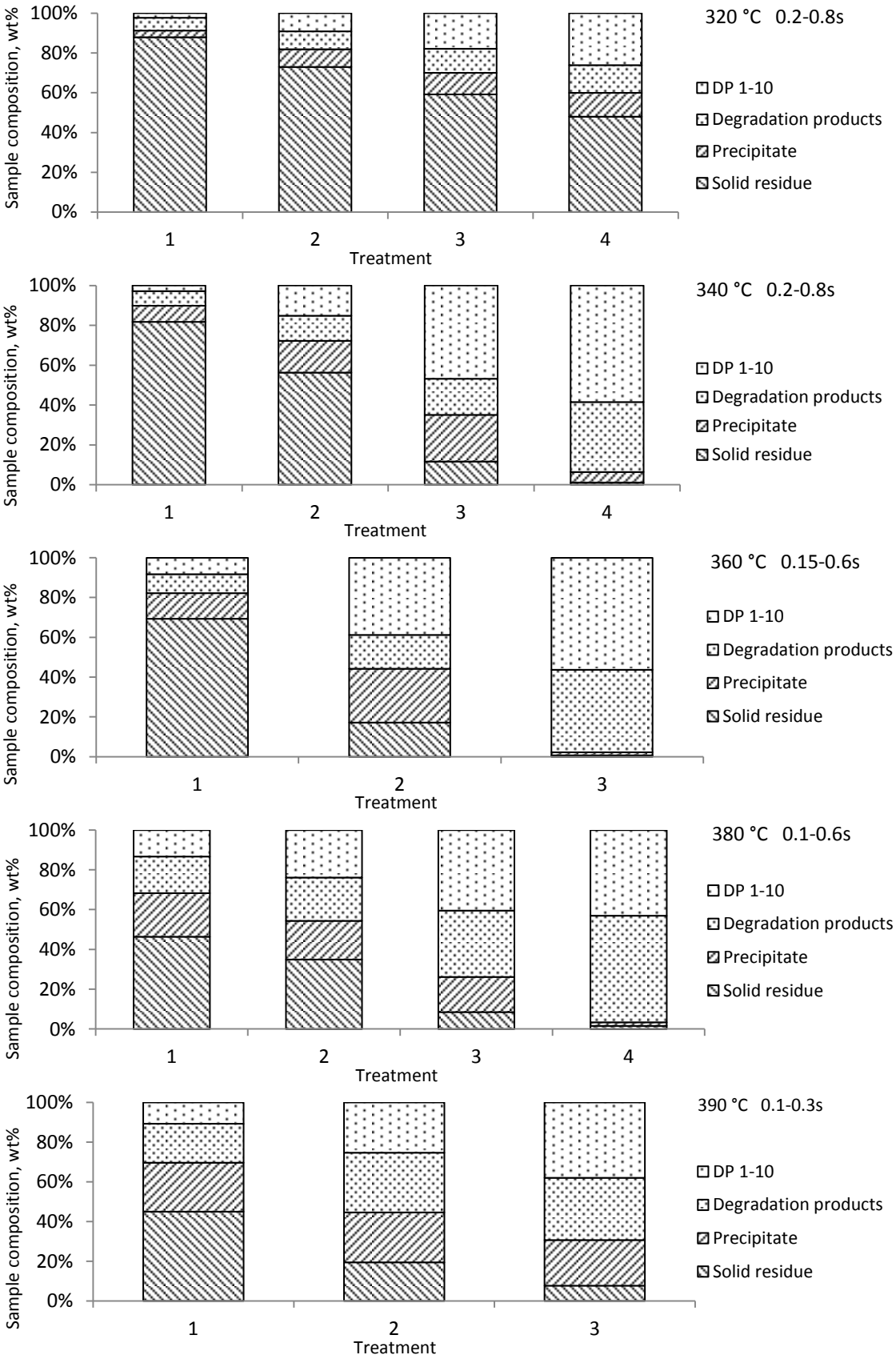

c) Product molar mass distributions, linear base

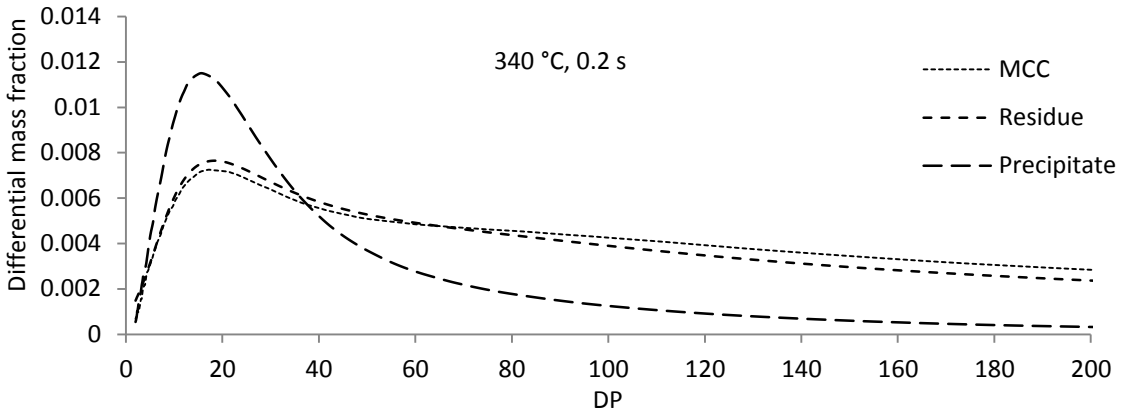

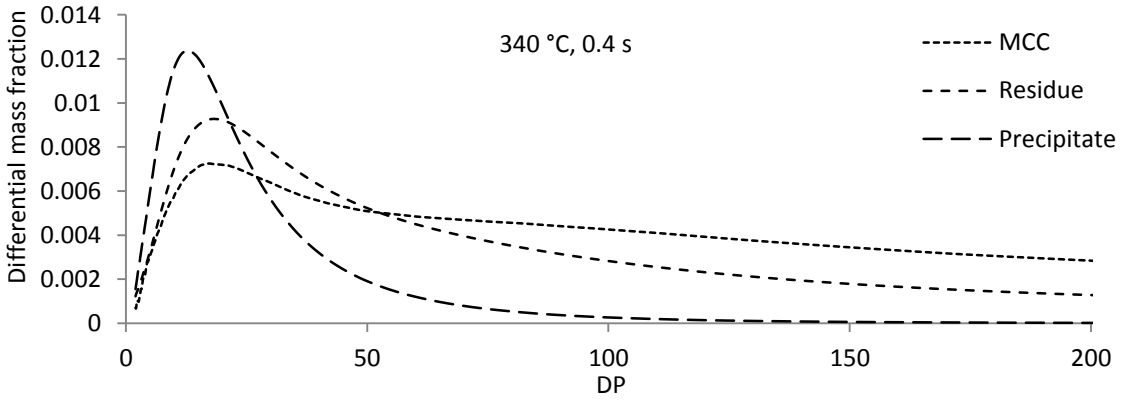

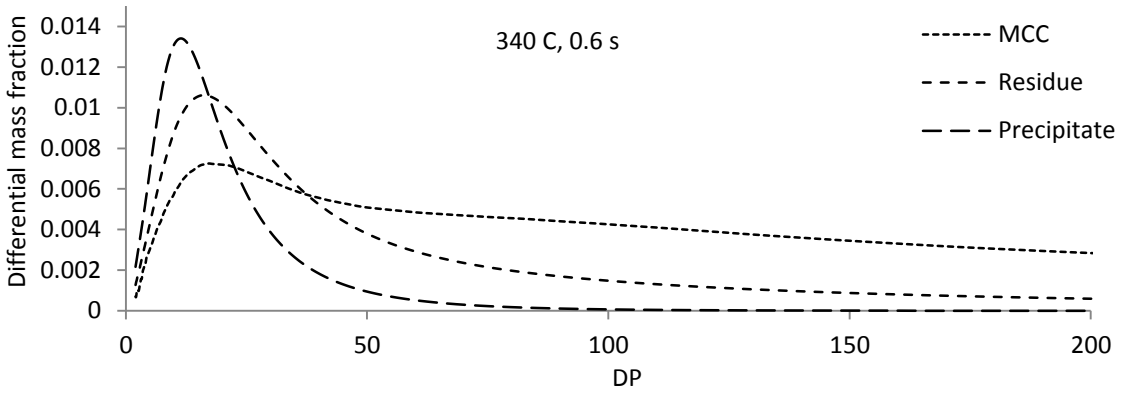

d) Product molecular mass distribution, logarithmic base

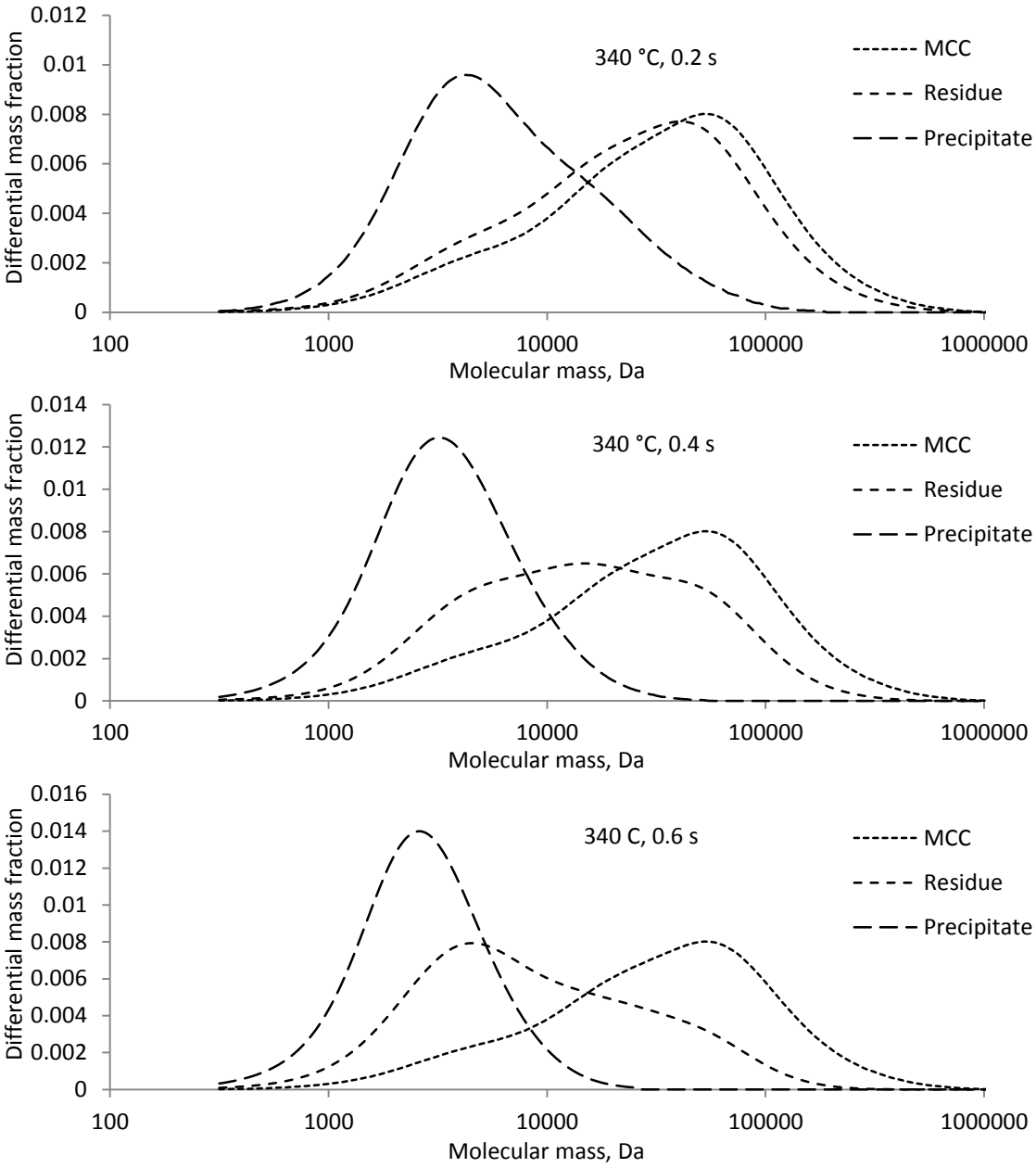

Appendix F: Techno-economic analysis

The following section describes the hypotheses, which were used in order to build a simple cost structure estimate of the process.

The selected operating parameters (related to SCWT and membrane ultrafiltration) for the techno-economic analysis are presented in Table 1. This analysis is based on the conversion of 1 kg of cellulose under the conditions which maximized the formation of water-soluble cello-oligosaccharides. Under these conditions the time required for the total conversion of 1 kg of MCC was 15 days of continuous operation.

Table 1. Selected operating parameters.

Step	Parameter	Value
SCWT	Temperature	360 °C
	Residence time	0.6 s
	Stock cellulose consistency	0.5 wt%
	cellulose : heating : quenching flow ratio	2:3:2
	Mass flow after reaction	2.0 kg/h
Ultrafiltration	Membrane MWCO	270 Da
	Mass flow	3.54 ml/(h.cm^2)

In addition to the design parameters a number of efficiencies have been estimated in order to describe the operations of real equipment. The selected efficiencies are presented in Table 2.

Table 2. Assumed process efficiencies.

Step	Component	Efficiency	Type
SCWT	Preheater	0.9	Electrical
	High-pressure pump	0.3	Electrical
Solid-liquid separation	Separation system	0.95	Mass fraction
Ultrafiltration	Glucose retention	50	Mass fraction
	Cellobiose retention	70	Mass fraction
	Cellotriose retention	80	Mass fraction
	Cellotetraose retention	80	Mass fraction
	Cellopentaose retention	80	Mass fraction
	Cellohexaose retention	80	Mass fraction
	Higher DP oligomers	50	Mass fraction
Ion-exchange column	Column separation	0.9	Mass fraction
Spray-drying	Spray-dryer	0.9	Mass fraction

Table 3 presents the experimental results at the selected operating conditions per unit mass of converted MCC. Table 3 also gives an estimated final yield according to the considered efficiencies.

Table 3. Estimated product yield.

Product	Gross yield after SCWT, g/kg MCC	Final process yield, g/kg MCC
Glucose	67.9	52.3
Cellobiose	71.7	55.2
Cellotriose	68.6	52.8
Cellotetraose	70.6	54.3
Cellopentaose	53.7	41.3
Cellohexaose	46.4	35.7
Higher COSs mixture	75.7	58.3
low DP cellulose II	10.7	9.7
Total valuable products	465.4	359.5
Residual cellulose	5.0	6.0
TOC in waste water	529.6	634.5

The table shows an overall product yield comprised between around 3.5 % and 5% for most individual product fractions, and a total yield of cello-oligomers and low DP cellulose (excluding glucose) around 30 %.

The assumed costs in terms of raw materials and energy input are presented in Table 4 according to the evaluated consumption (described in Section 3.2.8.) and returned to the processing of one kg of MCC. In addition, Table 4 presents the estimated potential for economies of scale in each component.

Table 4. Main estimated process operating costs.

Component	Indicative price	Consumption / kg of converted MCC	Total cost per kg of converted MCC	Potential for economies of scale
Microcrystalline cellulose	20 €/kg	1 kg	20 €	High
Electricity	154 €/MWh	403 kWh	57 €	Low
Water	4.18 €/m^3	1.4 m^3	6 €	Low
Ultrafiltration membrane	65 €/sheet (30 cm x 30 cm)	1 sheet (30 cm x 30 cm)	65 €	High
Total		153 €/kg of converted MCC		

The main process variable costs originate from electricity, microcrystalline cellulose, and ultrafiltration membrane. However, the displayed costs are valid for one kg of equivalent of treated MCC. It is believed that important economies of scale are possible for tangible materials, such as MCC and membranes. In addition, these estimations do not take into account any recovery of water or energy in the process, nor it includes potential process improvements, such as increased stock cellulose consistency.

The estimated capital costs related to the process are summarized in Table 5.

Table 5. Main estimated process capital costs.

Component	Estimated unit price, k€	Required quantity	Total price, k€
SCWT system	15	1	15
Solid-liquid separation	5	2	10
Ultrafiltration	5	1	5
Ion-exchange column	10	1	10
Spray-drying	5	1	5
Water purification	10	1	10
Automation and control	10	1	10
Utilities	5	1	5
Assembly	10	1	10
Total		80 k€	

This estimation does not include other significant costs related to the operation of the system, such as labor costs, real estate, logistics, maintenance costs, and the electricity consumption of utilities and equipment (such as pumps, mixing devices, replacement of ion-exchange resin, as well as automation and control systems) other than the main SCWT system.